THE ROLE OF PREDICTION IN CONTROLLING SMOOTH PURSUIT EYE MOVEMENTS OF CLEAR AND NOISY TARGET MOTIONS

By

JASON F. RUBINSTEIN

A dissertation submitted to the

School of Graduate Studies

Rutgers, The State University of New Jersey

In partial fulfillment of the requirements

For the degree of

Doctor of Philosophy

Graduate Program in Psychology

Written under the direction of

Eileen Kowler

And approved by

_____

_____

_____

_____

New Brunswick, New Jersey

January 2020

ABSTRACT OF THE DISSERTATION

THE ROLE OF PREDICTION IN CONTROLLING SMOOTH PURSUIT EYE MOVEMENTS OF CLEAR AND NOISY TARGET MOTIONS

by Jason F. Rubinstein

Dissertation Director:
Eileen Kowler

Smooth pursuit eye movements are used to maintain gaze on moving targets. In order to overcome processing delays, smooth pursuit is capable of predicting future target motion. While work over the years has characterized the nature of some of the cues (verbal, visual, probabilistic) to future motion, the integration of prediction with immediate sensory inputs is not well understood.

The current study tested the extent to which prediction during pursuit can be modeled as a form of optimal Bayesian cue combination, with prior and likelihood cues trading off in proportion to their respective reliabilities. Stimuli were random dot kinematograms (RDKs) consisting of 200 dots moving in a chosen mean direction with varying levels of directional variability (Gaussian, with SDs of 0, 30, 45, or 60 deg). The variability of the prior distribution determining the mean directions of the dots on each trial was also varied (Gaussian, with SDs of 10 or 45 deg, or uniform distribution from 0-360 deg). Subjects were instructed to pursue (pay attention to) the RDK and report the perceived mean direction of the RDK at the end of each trial.

The main experimental findings were: (1) The influence of the prior on pursuit persisted for ~250 to 600 ms after the onset of target motion. (2) The influence of the

prior decreased over time, with pursuit depending totally or near totally on the immediate stimulus motion (referred to as the "likelihood") by about 200-500 ms after the onset of target motion. (3) The influence of the immediate stimulus motion (likelihood) overcame that of the prior later in the trial when RDK directions were more variable. (4) Increasing the variability of the prior led to a greater influence of the likelihood on pursuit direction earlier in the trial. (5) When the variability of the prior direction increased, there were indications that the variability of the likelihood had a greater effect on the variability of pursuit directions. (6) Perceptual tests using short duration intervals of motion (150 ms) also found a greater influence of the prior and more variable reports of target direction when the variability of the RDK directions increased.

These findings suggest that basic principles of Bayesian cue combination can apply to smooth pursuit eye movements. These results can be useful for defining the quantitative characteristics of the cortical areas involved in both the representation of current sensory motion and the representation of the prior, as well as identifying the neural processes that are involved in the formation of the pursuit command via the combination of these two cues.

ACKNOWELDGEMENTS

I would like to thank my advisor, Eileen Kowler, for her unquantifiable level of guidance and training during the past ~7 years. When I joined the lab as an undergraduate REU participant summer 2013, I had no idea I would end up completing my doctorate here. It's amazing to me that the heart of the project I started on as a part of that program may live on. Enjoy all your tea!

I would also like to thank my committee members Manish Singh, Melchi Michel, and Bart Krekelberg for their useful comments and discussion after the defense, especially on the modeling details.

Thank you to Jie Wang for helpful discussion and moral support (in both research and CS classwork-related discourse) through the years. Best of luck finishing up over the next few years!

Thank you also to Morgan McCabe, Renee Tournoux, and Sameer Ahmad for both taking on a great deal of the subject running and offering helpful feedback on various aspects of the project.

Last but not least, thank you to my loving family for all your support throughout the past 6 and a half years as well as my entire life. Mom (Karen) and dad (Ron), I'll miss you out in California. And to my brother Adam – I'll see you out there soon! To our doggy, Peppermint Patty Rubinstein: you deserve all the pats in the world. Finally: rest in peace Mocha Rubinstein, who was very supportive by offering lots of licks through her 17.5 years of life.

TABLE OF CONTENTS

LIST OF TABLES AND FIGURES

Tables

Figures

1. Introduction

1.1. Background

Smooth pursuit eye movements are used to maintain gaze on smoothly moving objects. Classical models of smooth pursuit posit that the response is driven by low-level visuomotor signals that combine retinal slip velocity (the difference in velocity between the target and eye) with an extraretinal representation of eye velocity (Robinson, 1986; Lisberger, 2010). These two signals combined produce a representation of the target in craniotopic coordinates. If the signal is followed faithfully, the eye will match velocity with the target. However, a limiting factor is sensorimotor processing delay. Due to this delay, if a target changes direction abruptly, the eye would not keep up with the motion in the new direction, causing increased retinal error in the intervening period.

A general solution to this limitation, one that is found in visuomotor systems in general, is prediction. The concept of prediction is not unique to humans; even the salamander uses prediction to catch its prey. In a study by Borghuis & Leonardo (2015), for example, salamanders were shown to extrapolate the motion of a fruit fly in order to program effective prey-catching visuomotor actions. This leads the salamander to lash its tongue out to a position ahead of the current location of the fly. If the salamander were not able to predict, it would always miss any non-stationary fly and ultimately starve.

Smooth pursuit eye movements also predict, and the predictive capabilities extend beyond simple motion extrapolation. In classical studies, Westheimer (1954) and Dallos & Jones (1963) showed that the eye can change direction ahead of the target during pursuit of periodic (sinusoidal) motion.

Studies over the past 40 years have produced evidence that extended the predictive capabilities of pursuit beyond simple extrapolation of a straight-line motion path, and beyond predictive tracking of periodic motion, potentially involving higher-level representations of target motion. One example of such findings is anticipatory smooth eye movements (ASEM). ASEM occur when pursuit of constant velocity target motion begins prior to the onset of motion or prior to a change in the direction of motion (Kowler & Steinman, 1979, Westheimer, 1954). ASEM are also found when motion parameters are selected randomly, in which case ASEM are biased by recently seen or recently tracked target motions (Kowler & McKee, 1987; Kowler et al., 1984; Yang & Lisberger, 2012). In addition, cues (verbal or visual) induce anticipatory eye movements in the cued direction before the onset of target motion (de Hemptinne, Lefèvre, & Missal, 2006; Kowler, 1989, Santos & Kowler, 2017). Prediction during pursuit also occurs when moving targets are briefly blanked. In these instances, the eye tends to decelerate during the blank, but when the reappearance of the target is expected, the eye starts to re-accelerate prior to the reappearance (Becker & Fuchs, 1985), even when the target trajectory is curved (Orban de Xivry et al., 2008). Barnes & Collins (2008) showed that this acceleration occurs even when the target is blanked at the beginning of its motion. In this case, pursuit appears to be influenced by the velocity of the prior trials, implying that memory of motions can initiate pursuit even in the absence of an immediate motion signal.

These many demonstrations of predictive smooth pursuit require new models, ones that allow pursuit to be driven by more than low level visuomotor signals. In response to this need, some models of smooth pursuit, such as Barnes & Collins (2008),

proposed than an extraretinal signal containing information about prior target motions could be combined with the visuomotor signals to drive pursuit when purely visuomotor signals were not sufficient. In Barnes & Collins (2008), the extraretinal signal was controlled via a switch that turned prediction on or off at certain moments (such as when the target is blanked). However, others (eg. Orban de Xivry, 2013) have been critical of this approach and suggested instead that pursuit may depend on the relative weights of sensory and non-sensory cues, rather than an all-or-none "prediction switch".

More recent studies have attempted to test the idea that pursuit depends on a weighted combination of extraretinal information (including prediction) with current sensory signals. According to the principles of optimal cue combination (Ma, 2012; Trommershauser, Maloney, & Landy, 2003), greater uncertainty (and thus lower reliability) about the current sensory motion should result in a greater influence of the past history of motion (priors).

The following section describes three articles from the past 6 years which attempt to develop models of smooth pursuit eye movements that combine sensory (retinal) information and non-sensory (extraretinal) signals to drive pursuit in an attempt to account for the predictive and anticipatory aspects of pursuit outlined above. While these three studies involve discussion of Bayesian inference and weighted combinations of multiple cues, they vary in their approach and results, indicating there are still many gaps to fill in the understanding and modeling of anticipatory pursuit eye movements.

1.2. Bayesian models of pursuit

Some support for the idea that pursuit can be modeled as a form of cue combination, weighting prior and likelihood information in accordance with their respective reliabilities, came from Darlington et al. (2017), who analyzed and attempted to model the effects of context on the velocity and direction of eye movements in monkeys. Each pair of trials consisted of a prior-adapting trial, which varied on each trial, and a probe trial, which was always the same. Given an optimal combination of sensory inputs the prior (the first in the pair of trials) and the probe, it was expected that the effect of the prior-adapting trial would be modulated by the strength of the sensory signal on the probe trial. Based on findings that population responses in MT are weaker with lower contrast targets (Krekelberg et al., 2006), the strength of the sensory signal on the probe was manipulated by presenting the target in higher or lower contrast. The first of two main experiments analyzed speed context effects and the results confirmed their expectations, with more of a bias toward the speed of the prior-adapting trial on the probe trial for the low-contrast targets than the high-contrast targets. The second experiment found a similar effect of the prior-adapting trial on target direction, with the lower-contrast probe trials resulting in pursuit with more bias in the direction of the prior-adapting trial than the higher-contrast trials.

The explanation of these effects of context is that a lower-contrast target provides a “weaker” or “less reliable” motion signal, due to a relative decrease of the population of neural responses in MT (Yang et al., 2012), which the authors assumed resulted in a greater influence of a prior for slow target speeds as previously documented (Weiss, Simoncelli, & Adelson, 2002). If the brain is operating in a Bayesian way, this weaker

incoming sensory signal should result in greater weight for the prior trial more than a stronger, more reliable signal. Their model for adaptation of the direction and speed priors takes into account the previous trial, weighted by the stimulus reliability (contrast in their model), in the calculation of the "strength" of the visuo-motor transmission, which they define as "gain". However, they make it clear that the while the models are an attempt to understand how Bayesian inference might manifest itself from the known neural circuits of pursuit, the models are not Bayesian models. This is because, while described as "a vehicle for instigating priors", they state that the gain parameters in their model are explicitly not prior probability distributions.

Their first of two models outlined a relatively simple weighted enhancement of gain based on the prior trial's speed or direction and the current sensory likelihood. The current sensory likelihood was represented as a Gaussian centered on 0° with one of two values of σ, corresponding to the contrast of the motion signal and thus reliability:

$$\text{Sensory Likelihood} = G(0, \sigma_{\text{low/high contrast}})$$

Equation 1

The gain enhancement of the previous trial was similarly multiplied by a Gaussian centered on 0° with standard deviation σ. This stage worked similarly for both the direction and speed prior experiments:

$$\text{Gain Enhancement Direction} = \text{Amp}_{\text{direction}} \cdot G(0, \sigma_{\text{direction}}) + 1$$

Equation 2

$$\text{Gain Enhancement Speed} = \text{Amp}_{\text{speed}} \cdot G(0, \sigma_{\text{speed}}) + 1$$

Equation 3

(1 was added to the speed and direction to enhance the gain along a specific direction without "affecting gain in other directions")

The resulting posterior distribution allowed eye speed and direction to be predicted:

$$\text{Posterior} = \text{Sensory Likelihood} \cdot \text{Gain Enhancement}$$

The values of sigma and $\text{Amp}_{\text{speed/direction}}$ were fitted using a least squares approach to estimate values that best replicated the size of the effects in the experimental data.

Darlington et al. (2017) acknowledged that they were not the first to develop similar models of pursuit. Models by Orban de Xivry et. al (2013) and Bogadhi et al. (2013) both involved sensory and extrasensory components that were combined in a weighted sum based on their reliability in a way that is explicitly Bayesian. While Darlington et al.'s model of gain control resulted in a Bayesian-inference-like outcome, they made a point that it is distinctly not a Bayesian optimal model and that pursuit may not even be optimal. In fact, they pointed out that, according to Ma (2012), optimality is not a requirement for Bayesian inference, which is simply defined as "Making a decision about a state of the world based on sensory observations by computing a posterior distribution." Under Ma's definition, Bayesian inference can be optimal (in the selection of the maximum a posteriori that will minimize cost), probabilistic (in that it includes a

representation of the likelihood and prior along with their uncertainty), or both. However, the goal of Darlington et al. was to simply model how the neural system implements the tradeoff between current sensory information and history of previous trials, with no particular claim that this neural integration was optimal or even completely probabilistic, since the experiment only took into account two levels of uncertainty and did not posit a representation of the entire distribution of the prior and likelihood.

Thus, their main requirement for the system to exhibit Bayesian inference was to see an increased reliance (via direction or speed-selective gain modulation) on the prior when the likelihood (sensory info) becomes less reliable. But, as described, this reliance does not need to be optimal. Darlington et al.'s model is more concerned with capturing the gain control aspects underlying the pursuit system as previously evidenced in neural and behavioral findings than trying to demonstrate the optimality of the system. This is clear when looking at their experiments; they make no claims about the weighting of the prior/likelihood other than that it is affected by a binary (low contrast vs high contrast) manipulation of the likelihood.

However, other models of pursuit eye movements, such as Orban de Xivry (2013) and Bogadhi (2013), were concerned with the Bayesian-optimality of the pursuit system, with the reliability of their sensory and prior representations represented as distributions, rather than based on the presence of a high- or low-contrast stimulus.

Orban de Xivry et al. (2013) attempted to model both the predictive and sensory aspects of the pursuit system, integrating past history and incoming sensed information. Previous models, such as the one proposed in Barnes and Collins (2008), attempted to model pursuit by combining the predictive and visual aspects of the system using parallel

models with a mechanism that would switch to a memory-based pathway when there was an expectation of future target motion. Orban de Xivry and colleagues, on the other hand, constructed a coherent model that incorporated a memory-based prediction system along with the classical visual-motor pathway of smooth pursuit, without any switching components or disparate mechanisms that would only apply when prediction is required. This was accomplished using two pathways: one for the sensory processes and one for the predictive process. Each pathway used a Kalman filter to generate an estimate of the retinal error (retinal slip (RS) relative to the target motion) based on the difference between previous estimates and current observed value of RS. The estimates of retinal error were then combined, weighted by their uncertainty and used in the motion integration step to generate a motor command, which drives the eye movement.

At each time step, the section of the model prior to the "Motion integration" node aims to estimate the current retinal slip (the difference between the target motion and eye motion at the current time step *k*) using these two pathways, sensory and predictive. The sensory pathway starts with the target velocity and the eye velocity to calculate the retinal slip (RS_{det} in Figure 1 of Orban de Xivry (2017)). Additive and multiplicative noise is incorporated to simulate the noise present in the brain in areas such as MT and the signal. This results in the noisy estimate at time step *k* (RK_k^{Noisy}). From there, the model attempts to estimate the hidden variable $\widehat{RS}_{k+1}^{Sens}$, the estimate of the sensory retinal slip on the next time step, given the noisy estimate of the RS and the previous estimate ($\widehat{RS}_k^{Sens}$) using Kalman filtering (K_k) (Eq. 4). This estimate, along with the estimated variance, was used in the motion integration step. This estimation procedure is depicted in the below equation and flowchart in Figure 2 of Orban de Xivry et al. (2013):

$$\widehat{\mathrm{RS}}_{k+1}^{\mathrm{Sens}} = \widehat{\mathrm{RS}}_{k}^{\mathrm{Sens}} + K_k\left(\mathrm{RS}_{k}^{\mathrm{Noisy}} - \widehat{\mathrm{RS}}_{k}^{\mathrm{Sens}}\right) + \eta_k$$

Equation 4

The goal of the predictive pathway is to output the retinal slip that is expected 150 ms into the future. Similar to the sensory pathway, the predictive pathway used Kalman filtering to estimate the retinal slip. Rather than directly using the eye velocity at time *k* to calculate the RS, the predictive pathway uses an efference copy of the signal from the eye plant to estimate the velocity. This was then subtracted from the estimate of target velocity at time *k* from the previous trial to calculate the predicted RS ($\widehat{\mathrm{RS}}_{k}^{\mathrm{Mem}}$):

$$\widehat{\mathrm{RS}}_{k}^{\mathrm{Mem}} = \widehat{TV}_{k}^{\mathrm{Mem}} - \dot{e}_{k}^{\mathrm{eff}}$$

Equation 5

Each time step (k), the prediction (stored as an "Internal representation", depicted in the blue portion of Fig 1 in Orban de Xivry (2013))) was updated using Kalman filtering once again to estimate target velocity from the brain's noisy observation. This was done similarly as in Equation 4 in that a Kalman filter is used to update the internal representation ($\widehat{\mathrm{TV}}_{k}^{\mathrm{Pred}}$) based on the difference between the current prediction of target velocity ($\widehat{\mathrm{TV}}_{k}^{\mathrm{Pred}}$) and the current observation ($\mathrm{TV}_{k}^{\mathrm{Obs}}$).

$$\widehat{\mathrm{TV}}_{k+1}^{\mathrm{Pred}} = \widehat{\mathrm{TV}}_{k}^{\mathrm{Pred}} + B_{\mathrm{int}}u_k + K_{k}^{\mathrm{Pred}}\left(\mathrm{TV}_{k}^{\mathrm{Obs}} - \widehat{\mathrm{TV}}_{k}^{\mathrm{Pred}}\right) + \epsilon_k$$

Equation 6

The internal representation was used to update the representation of target motion stored in memory (with some noise). This in turn was used for the anticipation of the motion of future trials, but not the current trial, where the two δ terms represent normally-distributed multiplicative and additive noise, respectively:

$$\left(\widehat{TV}_{k}^{\text{Mem}}\right)_{\text{Trial } j+1} = \left(\widehat{\text{TV}}_{k+150}^{\text{Pred}}\right)_{\text{Trial } j}\left(1+\delta_{\text{mult}}^{\text{Pred}}\right) + \delta_{\text{add}}^{\text{Pred}}$$

Equation 7

This dynamically-updated representation in memory, along with the output of the sensory step, was used to drive pursuit in the motion integration step. The inputs of this step were optimally combined, weighted by their estimated reliability. This was done in a Bayesian way, such that the greater the variability of the input, the less of a role that component would play in the final estimate of retinal slip. This optimal weighting of current information and past experience is a key aspect of the model's ability to generate anticipatory smooth pursuit eye movements in testing, as it allows the system to increasingly rely on memory of previous trials' motion in situations where the current sensory information is not as reliable. After passing the optimally weighted estimate of retinal slip through the motion pathway, the signal is then sent to the motor system to initiate the eye movement.

The results of their simulation show that the model was able to exhibit many of the predictive and anticipatory properties of smooth pursuit present in human subjects. For instance, tracking a target moving with a sinusoidal velocity, the simulation took advantage of the periodic nature of the stimulus similar to the way humans do, lagging behind the target at first but quickly using the dynamically updated representations of the motion from the previous half cycle to anticipate the future motion (Figure 3 in Orban de Xivry (2013)). The model was also able to exhibit anticipatory smooth pursuit after repeating several trials of an identical motion, with the internal representation of the future target velocity building up. The system then uses this representation to initiate

smooth pursuit prior to the target motion, resulting in a movement in the anticipated direction of the future motion.

Their model also simulated the pattern of smooth eye movements also applied to instances of target blanking. Simulated smooth pursuit movements matched the behavior of experimental data undergoing the same kind of blanking of a moving target, indicating a prediction of the future movement of the target (an increase in gain in accordance with the previous trial's motion) based on the internal representation of the trajectory of the target.

Overall, this model was able to generate pursuit movements consistent with previous studies across several tasks and suggests that memory of previous trials is dynamic and combines optimally with current perceptual information. Orban de Xivry and colleagues argued the use of a Kalman filter allowed the model to update the memory dynamically using the noisy sensory inputs. While the performance of their model clearly exhibits the predictive properties of eye movements present in human observers, it does so only in qualitative comparisons to past research. The predictions clearly use information from previous trials in its "internal representation" of the target motion, integrated with the current sensory info, these predictions rely on parameters either obtained experimentally from previous studies or fit to the data. Other values, such as the gain of the pursuit system (G_{int}), were set a priori and either held constant or manipulated to demonstrate individual differences due to variability of residual pursuit in individuals. Additionally, most of the increase in "uncertainty" of the sensory information was in periods of target blanking; the sensory info was never granularly changed and tested. It was either there or not.

To be able to truly test their model, future iterations the model should be tested on situations in which the both the uncertainty of sensory information (representation of likelihood distribution) and built-up internal representations of previous trials (representation of prior distribution) are controlled. From there, it can be tested whether their model optimally combines information (weighted by uncertainty) in the same way the human system does. Additionally, recent experimental results have confirmed aspects of their model suggesting a buildup of a short-term memory representation of target motion over time, which integrates with the sensory representation of target motion as a function of the reliability of the prior and current sensory motion (Deravet, Blohm, Orban de Xivry, & Lefèvre, 2018), but this finding has only shown an influence on target speed, not direction.

Bogadhi et al. (2013) proposed a two-stage recurrent Bayesian model in the context of an experiment regarding the well-known aperture problem. One of the central issues of the aperture problem results when the early motion processing stage results in the perception of a tilted bar moving through an aperture (usually a small circular "window") as moving orthogonal to the orientation of the bar due to the ambiguity of 1-dimensional motion signals. Because of this, pursuit is biased to the direction orthogonal to the bar. 200 ms later, this bias is reduced once the 2-dimension motion signals come into play. But, as described earlier, in most pursuit tasks with uncertain sensory stimuli, these two motion signals are not the only inputs to the pursuit system. Extraretinal internal representations of prior motions have previously been successfully modeled in a recurrent fashion (Montagnini et al., 2007). The aperture problem paradigm is particularly suited for teasing out the underlying dynamics of prediction in pursuit due to

the well-known timecourse of the influence of the sensory information on the pursuit bias.

In this paper, Bogadhi et al. describe two experiments, where the target of pursuit is blanked either in the early phases of pursuit (first 100 ms) or the later, steady state stage, theorizing that the interaction between the retinal (sensory) and extraretinal signals changes depending on the time of stimulus blanking.

The integration of prior and likelihood during a pursuit task was previously shown in an open-loop smooth pursuit model (Bogadhi et al., 2011). The 2013 model extends this to a closed-loop, dynamic two-stage model. Both models combine the perceptual inputs and memory of prior motion in an optimal way, where each input is weighted by an amount inversely proportional to its uncertainty. They emphasize that the 2013 model captures the characteristic decrease in horizontal velocity during target blanking and the vertical eye velocity transient when the target reappears. This phase-dependent change in pursuit velocity is predicted to be due to a domination of extraretinal signals during the early stage (high prediction) and of retinal signals during the steady state (low prediction).

Bogadhi et al., 2013 discusses two experiments, each examining the interaction between retinal (sensory-based) and extraretinal. For the first experiment, targets were blanked during the steady state phase of pursuit (600 ms after stimulus onset, blanked for either 200 ms or 400 ms). In half of the blanked trials, the target appeared after blanking with a 90° shift in orientation, and in the other half the target's orientation did not change after reappearing. In Experiment 2, the stimulus was blanked at either 100, 120, 140, 160,

or 180 ms after target onset in 5/6 trials, with the last 1/6 of trials involving no blanking (used as a control).

The main results were that pursuit at the end of a blank during steady state pursuit (Experiment 1) show a clear directional bias (resulting from the aperture problem), and responses at the end of blanks occurring at the beginning (first 100 ms; Experiment 2) after the beginning of pursuit showed little or no bias in this regard. Additionally, the drop in horizontal velocity of pursuit appeared to increase as the length of the blank period increased in the steady state, which was coherent with previous findings. Finally, they found higher anticipatory velocity during early pursuit blanks (Experiment 1) compared to during steady state pursuit (Experiment 2).

To further examine the results and the involvement of the different levels of prediction/reliance of extraretinal signals, they developed a hierarchical model for pursuit and simulated it in different contexts (prediction low/high and blanking during steady state/early stages). The model is composed of two parts, retinal (sensory) and extraretinal (predictive), combined in a weighted fashion. Both parts of the model are "recurrent" in that the prior is initially set on 0 (in 2D velocity space) but continually updated every iteration of the model (at every instant) using the posterior distribution.

The inputs to this model were 1D (edge related, usually playing a larger role in the beginning of the motion) and 2D (terminator related, taking over later in the motion) likelihood distributions for the target motion. These values are combined and then fed to the retinal recurrent Bayesian network (the lower left box in Figure 9 in Bogadhi et al. (2013)). Here, the prior and likelihood (from the combined 1D and 2D signals) are combined using Bayes' rule to obtain the posterior distribution Q. At every timestep, the

posterior distribution is used to dynamically update the prior, which is used at the next iteration of the Bayesian network. A similar Bayesian network is used for the extraretinal block (Figure 9, top left in Bogadhi et al. (2013)). Here, the prior is combined with not the sensory likelihood but P_T, which is the probability of the target velocity in space. The sensory estimation Q and the prior of the extraretinal part P_{ext} are combined, weighted by their reliability, resulting in P_{out}. This is then combined with positive feedback to obtain P_T, the input to the extrasensory module. P_T not only updates the extraretinal prior but also is sent to the oculomotor plant to drive the actual pursuit movement.

This model is designed so that when the target is blanked, the likelihood is set to a Gaussian centered on zero with infinite variance. Thus, when the likelihood is combined with the prior, the posterior will be equal to the prior, which, due to the dynamic recurrent updating, will be gradually reset to its default setting of a Gaussian centered on 0. The MAP of the resulting posterior will be 0, so the estimated retinal velocity during the blank is 0. Therefore, the role of the extraretinal module is to have smooth pursuit continue, even when there is no sensory input.

Simulations of the model showed qualitatively similar pursuit responses obtained during high and low prediction phases, depending on when the target was blanked. In other words, the retinal variance appears to increase as the target is blanked and decrease when the target reappears. Even though the model's extraretinal variance remains relatively constant during the blank, the extraretinal weight is increased due to the relative difference in variance. The results of the model simulations led them to conclude that it was the level of prediction that determined the dynamics of pursuit during target blanking, irrespective of whether the blanking was during early pursuit or steady state.

Given the experimental data, this means that most of the subjects' responses involved low prediction in the steady state blanking and high prediction in early pursuit blanking.

The results show their model does offer a probabilistic cue combination framework integrating retinal and extraretinal representations of target information, weighted by their reliability, which qualitatively resembles the data from their aperture motion blanking experiments. Chiefly, it shows there is a correlation between the decrease in horizontal velocity during a blank and the bias in the vertical direction when the target reappears. However, as the authors admit, the model requires a lot of assumptions on parameters, namely the weight of the retinal signal, which is set to 1 at the initiation of pursuit and only changes during a blanking event. A more realistic model would have these weights being constantly updated during pursuit and not only depend on the blanking of the target. Additionally, the model, with only one free parameter (c, corresponding to the level of prediction), does not capture pursuit behavior for all subjects across the entire duration of pursuit, indicating a more flexible model may be necessary to account for the experimental data.

1.3. Summary and assessment

The models described above attempt to explain smooth pursuit predictive eye movements as a form of Bayesian cue combination and apply the principles of optimal cue combination in ways similar to the application found for studies of many aspects of perception (e.g., Kording & Wolpert, 2004; Ernst & Banks, 2002; Tassinari, Hudson, & Landy, 2006; Sato & Kording, 2014). This approach applied to smooth pursuit has resulted in two main achievements: (1) An experimentally-demonstrated influence of

context on smooth pursuit speed, with the effect of context becoming more prevalent on trials with lower target contrast (Darlington et al., 2017; Darlington, Beck, & Lisberger, 2018), and (2) computational frameworks which lay the groundwork for modeling the contributions of the prior (prediction) and likelihood (sensory) as a function of the uncertainty about the stimulus motion, with the expectation that the contribution of each is weighted according to their respective reliabilities, lending at least qualitative support for Bayesian optimal combinations of the two (Bogadhi et al., 2013; Orban de Xivry et al., 2013; Darlington et al., 2017).

However, there are still several unresolved issues if such Bayesian approaches are to be seen as fundamental to the understanding of pursuit:

(1) Costs: For observers to be considered to be "optimal" their actions need to minimize the expected cost of taking the action (Ma, 2012). This entails a specific cost function for different pursuit task trajectories task and a goal the pursuit system is trying to achieve. The goal of smooth pursuit has often been assumed to be match eye motion to target motion as closely as possible (minimizing retinal slip), but is this the only or most important goal? An analysis of costs and benefits of the particular might reveal that the best outcome might be something other than minimal (Rucci & Victor, 2015), or that a range of retinal motions would be acceptable. The goal of pursuit, and the role of retinal motion, may also change depending on the task.

(2) Implicit priors: The Bayesian models described in section 1.1 were based on priors derived from the past history of target motion. Pursuit, however, is also influenced by perceptual cues or implicit prior beliefs about target motion. Previous work has shown strong effects of perceptual cues on anticipatory pursuit, particularly cues that display the

path of motion of the target display consistent with geometry (Kowler, 1989; Santos & Kowler, 2017; Ladda, Eggert, Glasaur, & Straube, 2007). Consideration of such cues and implicit priors is needed to get a full understanding of predictive pursuit.

(3) Controlling of the uncertainty of the sensory motion: The work described in section 1.1 manipulated the uncertainty of the likelihood (the motion of the displayed stimulus) by either changing the contrast (Darlington et al., 2017) or completely blanking the stimulus during various stages of pursuit (Bogadhi et al., 2013). Contrast has been found to elicit weaker population responses in neural area MT (Krekelberg et al., 2006). However, contrast has been shown to affect the perceived speed of motion (Weiss, Simoncelli, & Adelson, 2002). A study of the influence of contrast on perceived direction, has not, to my knowledge, been done. An alternative way to manipulate directional uncertainty may be by using random-dot kinematograms, such as those used by Watamaniuk, Sekuler, & Williams (1989), Watamaniuk & Heinen (1999) and Mukherjee, et al., (2017). Watamaniuk et al. (1989) and Watamaniuk et al (1999) also found that an increase in the both the standard deviation of a Gaussian defining the local stimulus direction and an increase of the range of possible directions increased directional discrimination thresholds for both smooth pursuit and perceptual reports. The distribution of dot directions could thus be varied to control the level of uncertainty about the stimulus direction, which may be more transparent than manipulations of contrast. Alternatively, a “motion cloud” stimulus like the one used by Mukherjee, et al. (2015) could be used to vary the uncertainty of the stimulus motion without some of the idiosyncrasies of RDKs.

(4) Model parameters: The models of Orban de Xivry et al. (2013) and Bogadhi et al. (2013) estimated many parameters. Bogadhi et al. (2013) noted that their model required many assumptions about model parameters. The approach of Orban de Xivry et al. (2013) featured over a dozen parameters which were either estimated or taken from prior experimental findings. The large number of parameters is troublesome because it weakens the strength of conclusions that can be drawn about the process.

(5) Optimality: Assuming pursuit involves a Bayesian-optimal process of combining the prior and likelihood, the level of uncertainty of the sensory representation of the motion can be estimated using methods similar to Kording & Wolpert (2004) at each time interval of the motion. Additionally, this parameter could be estimated for multiple levels of prior standard deviation, with the prediction being if the prior and likelihood were truly integrated optimally and independently, the measure of sensory uncertainty should be consistent when only the prior is changed and not the likelihood at a given time interval. While prior work has suggested that pursuit may be operating optimally, none so far have tested for the independence of the optimal integration.

1.4. Current study

The present study, like the work reviewed in section 1.2, examined the extent to which a Bayesian cue combination of a memory-based prior and sensory likelihood, with each weighted according to their respective reliabilities, can account for the predictive aspects of smooth pursuit. This study attempts to address some of the gaps of the previous work:

(1) Stimuli were random dot kinematograms (RDKs) of a given mean and standard deviation, with the direction of individual dots selected from a Gaussian distribution on each frame. Thus, the relative variability of the stimuli was determined by the variability of the distribution of dot directions, not by contrast, or by the blanking of the target.

In addition, the mean (global) direction of the RDK on a given trial was selected from a Gaussian-distributed prior rather than a prior based on other context-based manipulations, such as the direction of the preceding trial or the motion properties of targets within a block of trials (Darlington et al., 2017).

(2) The relative roles of prior and likelihood (where "likelihood" refers to the distribution of dot directions of the RDK tested on any given trial) were examined over time to determine the timecourse of the influence of prior and likelihood on the direction of pursuit. Prior work, such as Darlington et al. (2017), looked at only one selected time interval.

(3) No procedures (e.g., randomized motion onset times as in Darlington et al., 2017) were employed to suppress anticipatory smooth eye movements (ASEM). ASEM are ubiquitous in pursuit (Kowler & Steinman, 1979; Westheimer, 1954; Becker & Fuchs, 1985; Kowler & McKee, 1987; Yang & Lisberger, 2012), and provide overt indication of the role of the prior. Suppressing ASEM may distort the effect of the prior in unknown ways.

(4) Perceptual estimates of the motion direction were obtained and compared with the properties of pursuit. This allowed for an assessment of psychophysical interpretations of the stimulus direction as it compared to the oculomotor response.

The central objective of the current study is to investigate how the predictive aspects of the smooth pursuit system may be influenced by the uncertainty of the immediate sensory information, and how the tradeoff of prior and likelihood distributions falls in line with the Bayesian cue combination approach used to describe many other perceptual and motor processes in the brain.

1.4.1. Motivation for the experimental design

The design of the present study was based on Kording & Wolpert (2004), who modeled the influence of prior history on motor localization as a function of the noise of visual feedback. In their task, subjects reached to touch a target in a virtual environment where visible feedback of the location of the finger was limited to a brief glimpse. This intermediate feedback was manipulated so that the position of a visible cursor representing the finger position was shifted relative to the actual position of the finger, and ample opportunity was given to learn the shift. The amount of the shift on any trial was sampled from a Gaussian distribution (prior). The noise of the intermediate visual feedback (likelihood) took on one of four values: infinite uncertainty (no feedback), clear (one small white sphere representing the cursor location), medium noise (25 small translucent spheres distributed around the cursor location with the standard deviation of positions set to 10 cm), or high uncertainty (25 small translucent spheres distributed around the cursor location with the standard deviation of positions set to 20 cm). Kording & Wolpert's (2004) goal was to determine whether pointing depended on a combination of the prior distribution of lateral shifts with the sensory information from the noisy visual feedback. Their main finding was that the noisier the visual feedback,

the more the endpoints of the reaches were biased to be closer to the mean of the prior distribution, a pattern of results consistent with a Bayesian strategy of weighting prior and likelihood in proportion to their respective reliabilities.

The current study also aimed to test the idea that Bayesian cue combination underlies the integration of sensory and extraretinal factors in smooth pursuit, involving a representation of the distribution of prior and likelihood along with their respective uncertainties. However, rather than a brief glimpse of sensory feedback provided during a reaching task, we varied the directional noise of the pursuit target, with the target remaining visible through the entire 1.5 s duration of the motion. Thus, the "feedback" was incorporated into the natural response of pursuit, where feedback is based on the sensed velocity or position of the retinal image. Note that these "sensed" velocities or positions used to control smooth pursuit could be represented at different levels of processing of the signal, or determination of the motor response, thus this study makes no initial assumptions about the level of representation, nor am I assuming that the representation of the variability of the stimulus is equal (quantitatively) to the variability of the motion of the dots on the screen.

1.4.2. Stimulus overview

The random dot kinematograms (RDKs) were generated using algorithms used in previous studies of RDKs (Watamaniuk & Heinen, 1999; Watamaniuk, Sekuler, & Williams, 1989; Mukherjee, et al., 2017) in that each dot's direction on every frame was sampled from a Gaussian likelihood with a mean (μ_L) and standard deviation (σ_L), and all dots were displaced in the chosen direction by the same amount. Using similar stimuli,

Watamaniuk, Sekuler, & Williams (1989) showed that the directional precision of pursuit of the motion decreased as the standard deviation of the directions composing the RDK increased. Watamaniuk & Heinen (1999) similarly showed that the precision of direction discrimination of pursuit depended on the standard deviation of RDK directions.

1.4.3. Analyses and expected results

On the basis of the previous studies described above, it was expected that: (1) before the onset of motion, the direction and speed of pursuit (ASEM) will be determined by the mean and standard deviation of the prior respectively; (2) the direction of later stages of pursuit will be determined more by the likelihood (the actual direction of the dots of the RDK); (3) the relative influence of the prior and likelihood on pursuit direction, including the timecourse of the transition of this influence, will depend on the relative variability of each (σ_P and σ_L).

To determine the relative influence of prior and likelihood, the direction of pursuit was compared to the mean direction of the RDK stimulus on any given trial. It was noted that the actual average direction of all the dots on each frame may differ from the nominal mean of the Gaussian which determined each dot's directions, but this difference was very slight, especially when averaging these directions across frames. Eye velocities were calculated during successive 100 ms windows (onsets separated by 1 ms) through the entirety of the 1500 ms trial. Scatterplots were prepared to show the actual direction of motion (defined by μ_L) on each trial vs. the direction of pursuit during a given interval of time, with separate scatterplots for different intervals of time. The influence of the likelihood on the direction of pursuit was then determined by the slope of the regression

line, where a slope close to 1 indicated close to full reliance on the likelihood, and a slope close to 0 indicated very little influence of the likelihood (and presumably high influence of the prior).

Slopes were determined separately for each tested level of σ_L. The influence of the prior was confirmed by the mean value of the pursuit direction, so a slope of near 0 and a mean value close to the prior would indicate full reliance on the prior. The main predictions were that (1) early in pursuit the prior will dominate, (2) the influence of the likelihood will increase over time, (3) the influence of the likelihood will be greater or emerge sooner for the clear ($\sigma_L = 0$) than for the noisy ($\sigma_L > 0$) RDK, (4) by some point in pursuit (for example, when it reaches steady state), the slopes would all be close to 1, showing complete influence of the immediate motion on pursuit direction.

After determining these slopes for different values of σ_L and time intervals, we will begin to investigate the plausibility of Bayesian cue combination using the method of Kording & Wolpert (2004). An analysis will be done to estimate the uncertainty in the likelihood under the assumption that the combination of the prior and likelihood is in proportion to their respective reliabilities. This will be achieved by adapting the approach used in Kording & Wolpert's (2004) Bayesian model. In my implementation of the model, the parameter representing the estimated uncertainty of the likelihood (σ_s) is not an estimate of the directional variability of pursuit (Mukherjee, et al., 2015) and is not be the same as the nominal noise of the distribution of directions in the stimulus (σ_L). Rather, the parameter (σ_s) controls the relative weight (compared to σ_P) assigned to the prior over the likelihood in the combination of the two cues, and presumably depends on both the noise of the distribution of dot directions (σ_L) as well as the time since the onset

of target motion. The value of σ_s will be estimated (as in Kording & Wolpert, 2004, and Yin et al., 2019) from the regression of the observed directions of motion as a function of the actual direction on each trial according to the following:

$$\theta_{t,n} = \frac{\sigma_s^2}{\sigma_s^2 + \sigma_P^2}\mu_P + \frac{\sigma_P^2}{\sigma_s^2 + \sigma_P^2}\mu_s + bias$$

Equation 8

where σ_P, μ_P, μ_s (the observed direction of the stimulus on a particular trial, μ_L), are based on the stimulus, and $\theta_{t,n}$ is the observed direction of pursuit at time interval t and trial n.

The thesis consists of 6 experiments.

1) Study of smooth pursuit with 3 levels of sensory noise: σ_L = 0, 30, or 45 deg, σ_P = 10 deg (Prior: N(μ_P, 10 deg), likelihood: N(μ_L, 0, 30 or 45 deg))
2) Study of smooth pursuit with 3 levels of sensory noise: σ_L = 0, 45 or 60 deg, σ_P = 10 deg. (Prior: N(μ_P, 10 deg), likelihood: N(μ_L, 0, 45 or 60 deg))
3) Study of smooth the variability of pursuit with 3 levels of sensory noise: σ_L = 0, 45 or 60 deg and a uniform prior (U(0, 360 deg))
4) Study of smooth pursuit with 3 levels of sensory noise and two values for RDK noise (5.3 deg/s and 6.36 deg/s).
5) Study of smooth pursuit with the low level of sensory noise (σ_L = 0) and two priors: σ_L = 0, 45 or 60 deg, σ_P = 10 or 45 deg. (Prior: N(μ_P, 10 or 45 deg), likelihood: N(μ_L, 0, 45 or 60 deg))
6) Study of perceptual discrimination of motion durations under instructed to fixate, with short (150 ms) presentations and with a noise mask before and after critical motion. σ_L = 0, 45, or 60 deg, σ_P = 10 deg (Prior: N(μ_P, 10 or 45 deg), likelihood: N(μ_L, 0, 45 or 60 deg))

2. Methods

2.1. Stimulus

Stimuli were displayed on a Dell M992 CRT Monitor (refresh rate 60 Hz; Dell, Round Rock, TA) viewed from a distance of 65 cm. Monitor resolution was set to 1280 x 1024 pixels (28.29 deg x 22.63 deg). Stimuli were presented in a fully lighted room, allowing the boundaries of the display region to be seen. Viewing was binocular and the head was stable in a chin rest.

2.1.a. Random dot kinematograms

Displays consisted of random dot kinematograms composed of 200 dots, each made of a 5 x 5 pixel (0.11 x 0.11 deg) square with luminance of 144.1 cd/m^2 on a background with a luminance of 3.55 cd/m^2. Dots were contained within a circular aperture with a radius of 450 pixels (10 deg). Initial dot x and y positions were uniformly sampled across this circular region at the beginning of each trial and displayed along with a center fixation cross. Extensive preliminary testing was done to confirm the selection of the number, speed, and luminance of the dots, and the radius of the display aperture, with choices largely dictated by practical considerations such as finding parameters so that at least 1.5 s of pursuit could be obtained without the eye reaching the edge of the screen.

Each dot's direction on each frame was sampled from a Gaussian distribution with a given mean (μ_L) and standard deviation (σ_P). Different levels of σ_L were tested, effectively manipulating the noise of the sensory likelihood for each trial (see section 3). Figure 0.1 shows an illustration (using large dots for the purposes of illustration in the

figure) of one of frame with a clear ($\sigma_L = 0°$) and noisy ($\sigma_L > 0°$) stimulus, with the arrows indicating the mean direction of the dots on the frame.

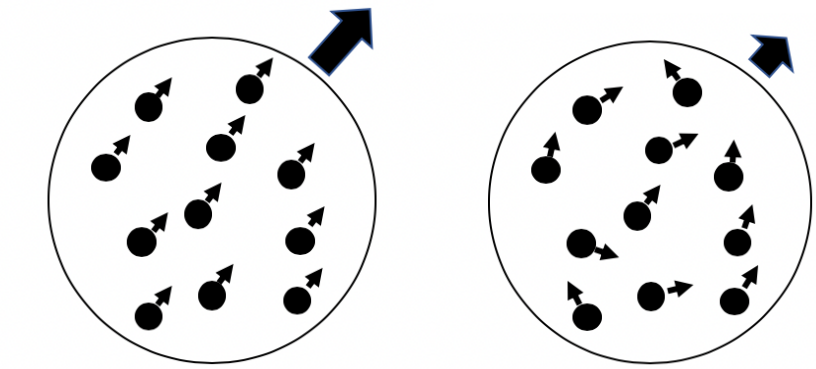

Figure 0.1: Sample RDK stimuli. Left: Illustration of a "clear" ($\sigma_L = 0$) stimulus, with all the dots moving in the same direction (μ_L). Right: Illustration of a "noisy" ($\sigma_L > 0$) stimulus, with dots moving in a wider range of local directions, but with the same mean (global) direction (μ_L).

The value of μ_P and σ_P were constant for all experimental sessions for a given subject. The value of μ_L was sampled from the prior distribution ($N(\mu_P, \sigma_P)$) on each trial. The value of σ_L for the noisy trials varied depending on the experimental session. On each frame, each dot was displaced in the selected direction (sampled from the prior distribution) an amount determined for each subject and each level of σ_L (see section 2.1b). The dots continued moving in this fashion for 1.5s (90 frames). Dots had infinite lifetime and were displaced to the opposite end of the circular aperture when they reached the edge of the circle.

2.1.b. Choosing the directions of the prior

To select the direction of the prior (μ_P), a preliminary session was run in which the mean direction of dot motion (μ_L) on each trial was randomly selected from four different oblique directions (45, 135, 225, 315 deg). This session only contained clear ($\sigma_L = 0°$) trials. The direction that appeared to elicit the greatest mean speed of pursuit for each subject was chosen as the prior mean (μ_p). In some cases, μ_p was shifted slightly (5-10°) away from the chosen direction since those were less salient than directions 45 degrees from the cardinal directions.

2.1.c. Speed scaling

The average speed of an RDK decreases with increased variance of the distribution of dot directions (Groh et al., 1997). To equate speeds between clear and noisy RDKs, the amount of displacement per frame for the different levels of σ_L was determined empirically (Heinen and Watamaniuk, 1999; Mukherjee et al., 2015). This was done in preliminary sessions where the prior standard deviation (σ_P) was set to be 0°, so that the mean direction of dots on each trial was always the same. Different displacements per update were tested to find values in which the steady state eye speeds for each value of σ_L were approximately equivalent. The chosen stimulus speeds which resulted in a match for the steady state speeds did not necessarily equate earlier in pursuit. A control experiment involving two different speeds for the clear ($\sigma_L = 0°$) stimulus was run to assess whether a change in solely the speed of pursuit would affect the timecourse of the relative influence of prior and likelihood on pursuit direction.

2.2. Procedure

2.2.a Smooth pursuit

Each trial began with a fixation cross in the center of the display. Subjects were instructed to blink a few times, fixate the center cross, start the trial by clicking the mouse button, and pay attention to the motion of the dots. This instruction to pay attention to the motion is effective in eliciting brisk pursuit (e.g. Santos & Kowler, 2017). After the mouse click the fixation cross disappeared, leaving the static array of randomly-positioned dots. After 1 s, the motion began (section 1a). 1.5 s later, after the motion ended, the dot display was extinguished and replaced by a display used to collect a perceptual report of motion direction (Figure 0.2). This perceptual response was included to motivate attention to the RDKs. The display used to report this direction (via Method of Adjustment) consisted of a 225 pixel (5 deg) radius circle (luminance: 144.1 cd/m^2) with a white line extending from the center of the circle to the edge. The direction of the line was initially set randomly, and the subject adjusted the direction using the mouse. The subject was told to choose the direction that the dots moved. After selecting the direction, they clicked the mouse to record their selection. On the clear ($\sigma_L = 0°$) trials, feedback (via a blue line) indicated the nominal mean direction of the RDK on that trial. After the feedback was briefly displayed, the next trial began.

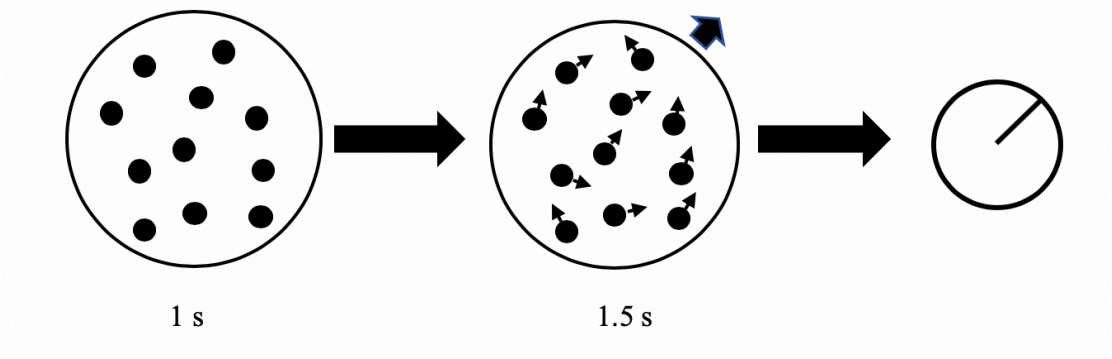

Figure 0.2: Sequence of displays on each trial. After fixating a central cross (displayed with a static dot field), participants clicked the mouse button. The static dot field remained for 1 second, after which the critical frames of stimulus motion occur. Finally, the participant used the mouse to move the pointer to the direction they saw the dots move and clicked the mouse, advancing to the next trial.

2.2.b. Perceptual estimates of motion direction: brief displays

Separate sessions were used to determine perceptual estimates of RDK direction without the influences of sustained smooth pursuit eye movements. The duration of motion was reduced to .15 s, a value too brief to elicit smooth pursuit near target velocity (Kowler & McKee, 1987). The very brief stimulus presentation not only decreased the available temporal information about the stimulus motion but also reduced the magnitude of any smooth pursuit that might result from the viewing (Pursuit velocities are low for brief stimulus durations; Kowler & McKee, 1987). The procedure was as follows. After clicking the mouse, a 1 s period of static dots were displayed as before. Next, a mask consisting of dots moving in uniformly random directions (0-360°) moved for 30 frames (.5 s). During this mask period, half of the dots moved at the same local speed chosen for the noisy trials and the other half moved at the speed of the clear trials. Then, the stimulus was blanked for 2 frames, followed by the critical period consisting of dot motion identical to the main experiment, lasting for .15 s. After this, the stimulus was once again blanked for 2 frames, followed by the same noise mask as before for .5 s. The

psychophysical response at the end of the trial was taken as described in 2.2.a.; however, no feedback to the actual mean direction of the RDK was provided.

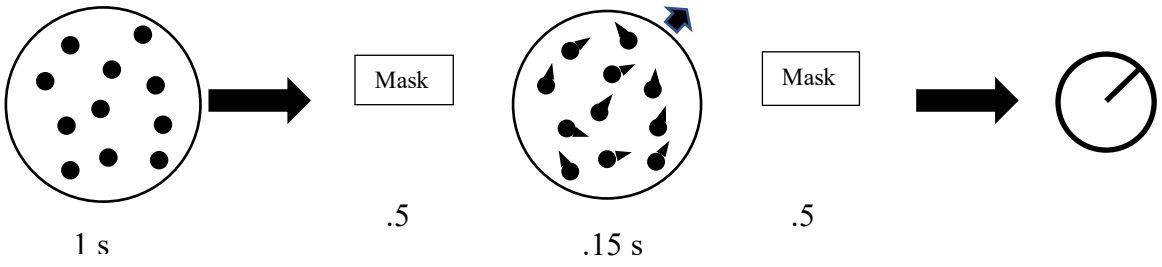

Figure 0.3: Sequence of displays on each trial for the perceptual condition. After fixating a central cross (displayed with a static dot field), participants clicked the mouse button. The static dot field remained for 1 second, after which a mask of random dots was displayed for .5 s. Then, the dots disappeared for 2 frames. Next, the critical frames of stimulus motion occurred. The dots were blanked for 2 frames again, followed by another .5 s mask. Finally, the participant used the mouse to move the pointer to the direction they saw the dots move and clicked the mouse, advancing to the next trial.

2.3. Design

There were 6 main experiments. The parameters of the experiments were outlined as in Table 1.

In the main experimental sessions (after the preliminary sessions described above and with the exception of Experiment 6, which only involved clear ($\sigma_L = 0°$) trials), each trial was randomly chosen to be either "noisy" ($\sigma_L > 0°$) or "clear" ($\sigma_L = 0°$) with a 50% probability of clear, and a 50% probability of noisy, which was set to a particular value of σ_L depending on the experimental session.

The table below indicates the various conditions that were run. "Pursuit" in the first column indicates the pursuit trials (1.5 s), whereas "Perceptual" indicates the shorter-duration perceptual trials (described in Section 2.2.a).

Table 1: Design of each experiment.

Experiment 1:

4 subjects

Task	**σ_P (deg)**	**σ_L (deg)**	**Approximate number of trials**
Pursuit	10	30	~750 trials
Pursuit	10	45	~750 trials

Experiment 2:

5 subjects

Pursuit	10	45	~750 trials
Pursuit	10	60	~750 trials

Experiment 3:

3 subjects

Pursuit	Uniform (0-360 deg)	45	~750 trials
Pursuit	Uniform (0-360 deg)	60	~750 trials

Experiment 4:

4 subjects

Pursuit	45	45	~750 trials
Pursuit	45	60	~750 trials

Experiment 5:

3 Subjects

Pursuit	10	0 (with RDK speed used in experiments 1-4 (6.36 deg/s))	~750 trials
Perceptual	10	0 (with slower RDK speed (~5.3 deg/s))	~750 trials

Experiment 6:

5 Subjects

Perceptual	10	45	~750 trials
Perceptual	10	60	~750 trials

Table 2: Percentage of samples omitted from analysis due to saccades across the timecourse of analysis (from -50 to 700) for Experiments 1 and 2 (number in parenthesis represents the total number of trials run in each condition). Note that a saccade lasts multiple time intervals, so multiple samples would be eliminated during a given saccade.

Experiment 1

Subject	**σ_L = 0°**	**σ_L =30°**	**σ_L =45°**
EL	24.01 (875)	25.21 (425)	20.36 (450)
JG	4.41 (700)	6.09 (275)	2.97 (425)
KP	24.48 (675)	23.17 (250)	18.06 (425)
BR	18.34 (300)	17.86 (150)	8.04 (150)

Experiment 2

Subject	σ_L =0°	σ_L =45°	σ_L =60°
AP	7.67 (625)	3.06 (350)	3.63 (275)
EL	23.11 (775)	21.07 (450)	7.74 (325)
JG	4.29 (850)	2.97 (425)	1.79 (425)
KP	21.3 (750)	18.06 (425)	12.39 (325)
WW	19.55 (775)	16.95 (350)	15.79 (425)

3. Results

3.1. Experiment 1

Experiment 1 compared pursuit of RDKs with three levels of directional noise (σ_L = 0, 30 or 45 deg). Trials with the clear RDKs (σ_L = 0°) were randomly interleaved with the trials with the noisy RDKs. Three subjects, (JG, EL, and KP) were tested in 10-17 50-trial blocks for the 30° and 45° values of σ_L. Subject BR was tested in 6 blocks for each value of σ_L. Preliminary testing was done to select the mean direction of the prior (μ_P) and the speeds of the different values of σ_L (see also Section 2.1.b). These results will be described first, followed by some basic properties of the observed smooth pursuit (mean eye speed, mean direction), and finally, the results of the analyses done to determine the relative influence of prior and likelihood on the direction of smooth pursuit over time.

3.1.1. Preliminary tests to select the mean direction of the prior

A. 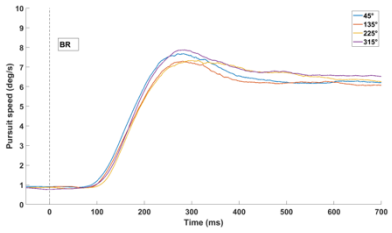

B. 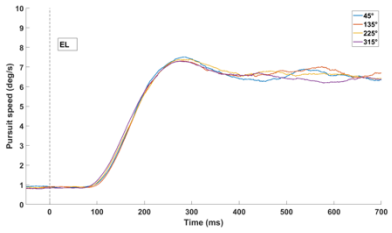

C. 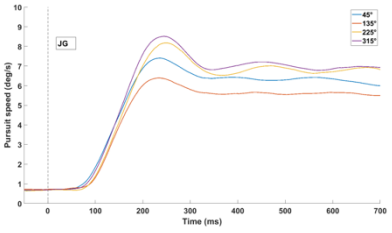

D. 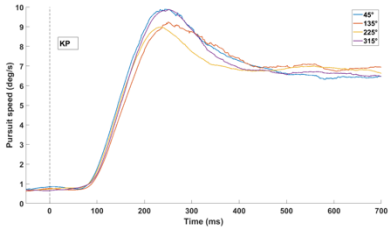

Figure 1.1 A-D: Mean pursuit speed over time for the 4 oblique directions (45, 135, 225, 315) for all 4 subjects. Time = 0 corresponds to the onset of stimulus motion.

In order to determine the mean direction of the prior (μ_P) the speed of pursuit was examined for RDKs moving in four oblique directions (45, 135, 225, 315 deg) for each of the 4 subjects in a preliminary set of sessions using the clear RDK ($\sigma_L = 0°$). The direction of motion was chosen randomly on each trial from the four oblique directions. The oblique direction that elicited the fastest pursuit at steady state was chosen to be that subject's μ_P. There was no important reason for choosing the direction that elicited faster speed, except perhaps to increase the signal/noise ratio. If multiple directions elicited similar pursuit speeds, μ_P was chosen arbitrarily. Figure 1.1 shows the mean speed of pursuit over time for each of the 4 subjects. The chosen values of μ_P were 315° for BR, 135° for EL, 315° for JG and 45° for KP.

Given that direction was chosen randomly, there were no prominent anticipatory smooth eye movements (ASEM) prior to the onset of target motion in the average direction traces (Santos & Kowler, 2017; Kowler et al., 2014).

3.1.2. Pursuit of RDKs: Speed and direction

This section will summarize some basic properties of the smooth pursuit of the RDKs whose mean direction on each trial was chosen from a Gaussian-distributed prior (μ_P, σ_P). The parameter μ_P for each subject is noted in section 3.1.1 and σ_P was set to 10°.

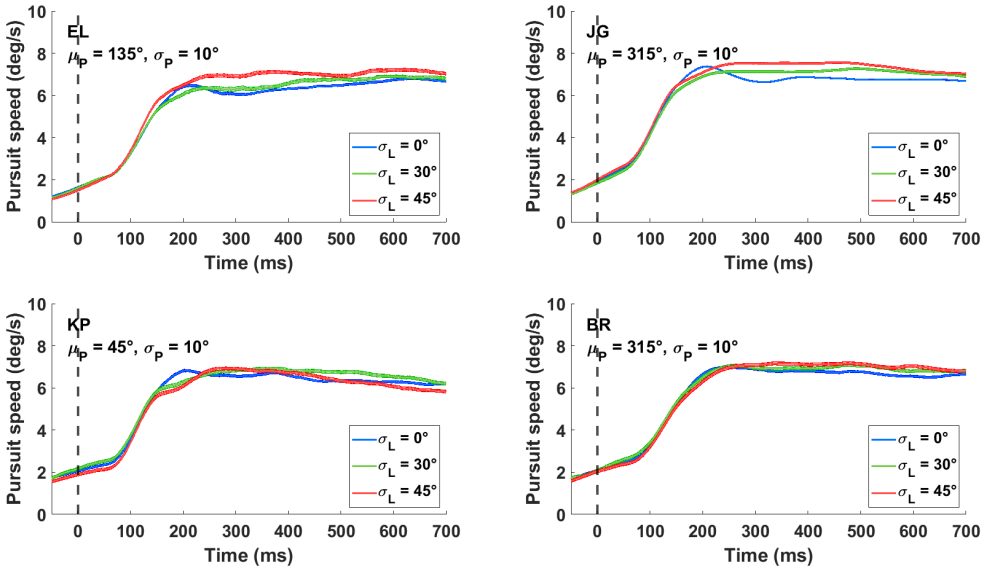

Figure 1.2 A-D: Mean pursuit speed (±SE) over time for each value of σ_L for each of the 4 subjects. Time = 0 ms corresponds to the onset of stimulus motion. Each line corresponds a level of σ_L. For all subjects, the speed of the dots on the clear trials was set to 6.4 deg/s. When $\sigma_L = 30°$, the speeds were as follows: BR, EL, JG: 8.0 deg/s. KP: 8.35 deg/s. When $\sigma_L = 45°$, the speeds were: BR: 10.3 deg/s, EL: 11.1 deg/s, KP: 10.6 deg/s, JG: 10.6 deg/s.

Fig 1.2 shows average eye speed over time for $\sigma_L = 0°$, 30°, and 45°. Eye speed was computed for successive 100 ms intervals whose onsets were separated by 1 ms. The speed of the RDK for each σ_L in pixels/display update (with update frequency 60 Hz) was varied in order to approximately equate eye speeds across the three levels of σ_L (Section 2.3). Fig. 1.2 confirms that eye speeds with the chosen number of pixels/update were approximately the same for all three values of σ_L.

Anticipatory smooth eye movements can be seen in Fig 1.2, as shown by the increase in eye speed prior to motion onset (Kowler et al., 2014). Eye speed increased at a higher rate about 100 ms after the onset of motion, showing the influence of the sensory motion after the typical pursuit latency (Carl & Gellman, 1987). Eye speed reached the approximate speed of the RDKs at about 200 ms after the onset of motion, a value expected from previous reports (Kowler & McKee, 1987; Robinson et al., 1986). The eye speed at 200 ms or later will be referred to as steady-state pursuit in keeping with conventional language.

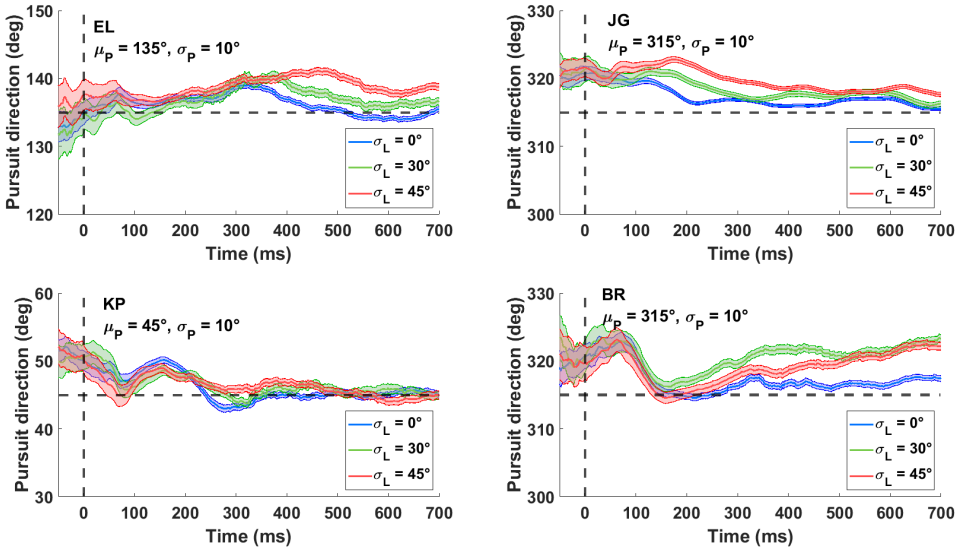

Figure 1.3 A-D: Mean pursuit direction (±SE) over time for each value of σ_L for each of the 4 subjects. Time = 0 ms corresponds to the onset of stimulus motion. Each line corresponds to a level of σ_L. The horizontal dotted line on each plot denotes the mean of the prior (μ_P) for that subject.

Mean pursuit direction over time is shown in Fig. 1.3. Mean direction for each 100 ms time interval was computed from the measured eye velocities using the circular mean functions from the CircStat MATLAB package (Berens, 2009). Note that the average direction of ASEM prior to target motion onset was close to each subject's

respective μ_P, confirming that that the direction of the prior mean, μ_P, had been learned. Mean direction later in pursuit, averaged over all trials regardless of the actual direction on that trial, remained close to μ_P. The effect of the actual direction of RDK motions on a given trial is considered in 3.1.3.

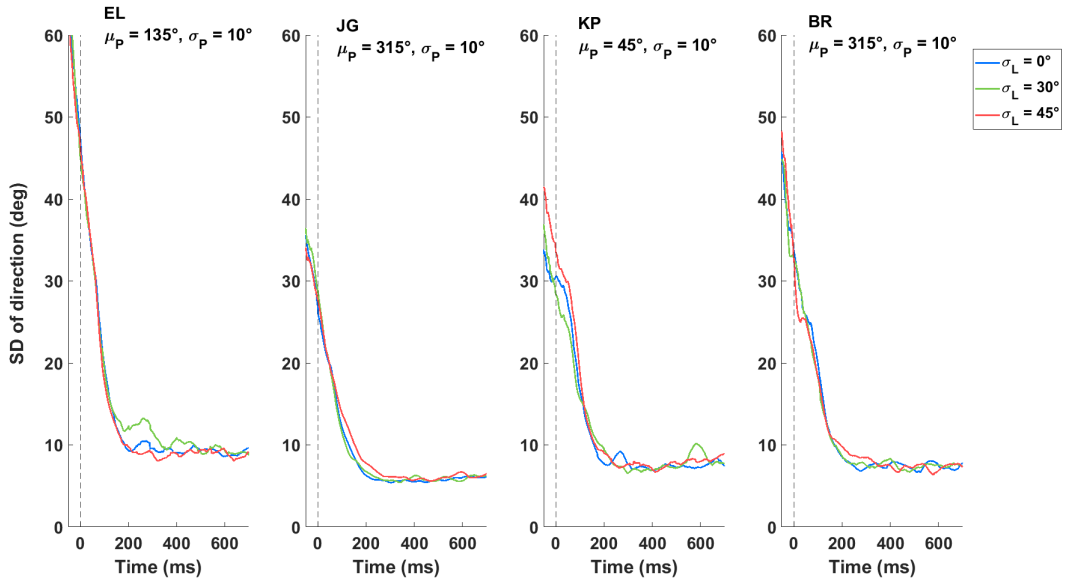

Figure 1.4 A-D: The standard deviation of pursuit direction over time for each value of σ_L for 3 subjects. Time = 0 ms corresponds to the onset of stimulus motion. Each line corresponds to a level of σ_L.

Figure 1.4 shows the SDs of pursuit directions. SD was computed by first subtracting the observed direction of motion in each time interval from the actual direction of RDK target motion on that trial. Figure 1.4 shows that SDs decreased over time, as eye speed increased (Fig 1.2) with SDs reaching lowest values about 200 ms after the onset of target motion, when steady state eye velocity was reached. The high values of the directional standard deviation (prior to 200 ms) is associated with the slower pursuit speeds. The SDs did not differ appreciably for the different levels of σ_L through

most of the trial. This was confirmed via tests of homogeneity of variance (Bartlett's test), with p values well above 0.05 throughout the trial (Fig 1.5). SDs of eye direction will be considered again in section 3.3 where SD's will be presented for a situation where the direction of motion was selected from wider directional intervals.

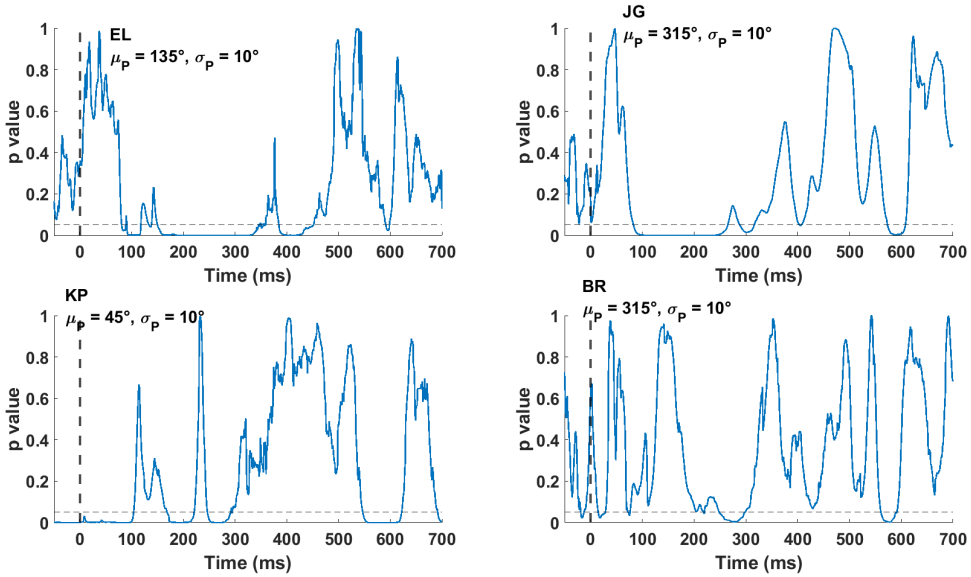

Figure 1.5 A-D: Resulting p value from Bartlett's test of homogeneity of variance, computed for the 3 levels of σ_L over the timecourse of the trial. Time = 0 corresponds to the onset of stimulus motion. The horizontal line indicates a p value of 0.05. Each function is based on about 150-450 trials for the noisy (σ_L = 30° and σ_L = 45°) trials and about 300-900 trials for the clear (σ_L = 0°) trials.

3.1.3. Influence of prior and likelihood over time

The next set of analyses addresses the central objective of the project, namely, to determine the relative influence of two factors, the actual target motion (likelihood), and the direction conveyed by the prior (μ_P), on the observed direction of pursuit over time.

Fig 1.6 shows examples of scatterplots of the observed direction of pursuit direction vs. the direction of target motion for three different time intervals: 150 ms, 300 ms, and 415 ms after the onset of target motion. Slopes of the best fitting straight lines are shown for each scatterplot. Fig. 1.6 shows that the slopes increased over time. In

addition, the mean direction of pursuit was close to the direction of the prior. These results illustrate the change over time from pursuit depending mainly on the prior to pursuit depending more on the actual direction of target motion (likelihood). The shallow slopes at earlier times were due to higher directional variability (Fig. 1.4). High directional variability of pursuit direction influences the scatter of values around the best fitting straight line, rather than the slope (this was verified by simulations).

A. T = 0, σ_L = 0. Slope = 0.0433.

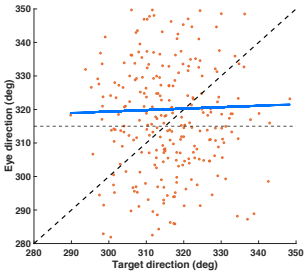

B. T = 150, σ_L = 0. Slope = 0.472

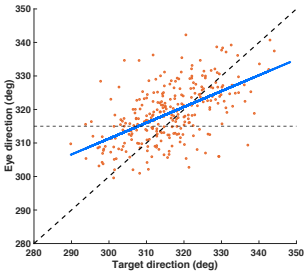

C. T = 300, σ_L = 0, Slope = 0.9463.

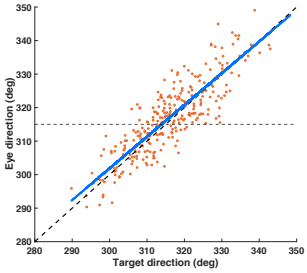

Figure 1.6 A-C: 3 example scatter plots of μ_L vs. pursuit direction on each trial. Each dot represents one trial for the given time interval (Time = 0 ms corresponding to the onset of target motion). The horizontal dotted line shows the expected results if pursuit solely used info from prior (pursuing only μ_P). The diagonal dotted line shows the expected results if pursuit solely used info from likelihood (pursuing only μ_L). The solid blue line was obtained via linear regression from the data. The time displayed above each graph indicates the time after motion onset the scatterplot represents.

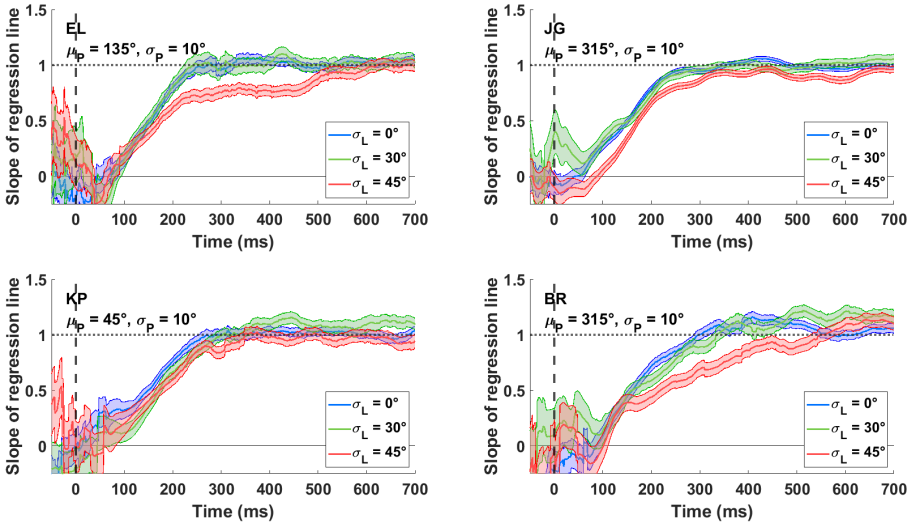

Figure 1.7A-D: Slope of regression line relating target (μ_L) and eye direction (± SE) on each trial over time. Time = 0 ms corresponds to the onset of stimulus motion. Each line represents a different level of σ_L.

Figure 1.7 shows slopes as a function of time (± standard error) for the different levels of σ_L. Three trends are apparent. First, as expected, slopes were initially shallow and quite variable until 100 ms following the onset the onset of the motion, when the influence of the immediate sensory motion began. Second, slopes gradually increased to values close to 1 over time, showing that pursuit direction increasingly reflected the influence of the direction of the current trial's stimulus motion over time. Third, the rate of the increase of the slope, as well as the maximum value of the slope, depended on the level of σ_L. For $\sigma_L = 0$ deg and $\sigma_L = 30$ deg, slopes reached values near 1 about 250-300 ms after the onset of target motion. When $\sigma_L = 45$, slopes reached values near 1 later, about 350 to 600 ms after the onset of target motion. Note that for all values of σ_L, slopes did not reach their highest values until well after pursuit reached steady state speeds (see Fig. 1.2), suggesting that the rapid acceleration of the eye during initial portions of pursuit was driven in part by the prior. Figure 1.7 also shows that results were quite

similar for σ_L = 0° and 30°, suggesting the noise of the RDK when σ_L = 30° was not great enough to overcome the internal noise of the pursuit. (Analysis of the statistical significance of the difference in results for the different levels of σ_L will be considered in the following sections.)

3.1.4. Estimating the relative role of prior and likelihood

To investigate the plausibility of the relative role of prior and likelihood manifesting as a form of Bayesian cue combination, the optimal estimate may be expressed as a reliability-weighted combination of prior and likelihood (Kording & Wolpert, 2004) (Eq. 8), which was summarized in section 1.4.2.

$$\theta_{\mathrm{t,n}} = \frac{\sigma_{\mathrm{s}}^2}{\sigma_{\mathrm{s}}^2 + \sigma_{\mathrm{P}}^2}\mu_{\mathrm{P}} + \frac{\sigma_{\mathrm{P}}^2}{\sigma_{\mathrm{s}}^2 + \sigma_{\mathrm{P}}^2}\mu_{\mathrm{s}} + bias$$

Eq. 8

θ_t represents the estimated direction of pursuit at time interval t and on trial n. The mean (μ_P) and standard deviation (σ_P) of the prior were assumed to be the same as the actual parameters used in the experiment, an assumption also made by Kording & Wolpert (2004) and supported in part by the closeness of the ASEM direction to the mean of the prior. Eq. 8 also includes a parameter, σ_s, which, along with the nominal standard deviation of the prior (σ_P) represents the effective weight on the prior over the likelihood ($\frac{\sigma_{\mathrm{P}}^2}{\sigma_{\mathrm{s}}^2+\sigma_{\mathrm{P}}^2}$). The value of σ_s will be estimated by fitting the model (Eq. 8) to the observed direction of pursuit at each time interval. An additional parameter to represent a net offset (bias) of pursuit direction was also included to capture possible directional biases of pursuit that would be internal to the system and unrelated to stimulus condition. The

main predictions were that the level of σ_s obtained from fitting the model will decrease over time (as the slopes in Fig 1.7 increased) and will be larger for the noisier likelihoods. These predictions reflect (at least qualitatively) the key idea in Bayesian cue combination, which is that the relative weight of the contribution of prior and likelihood depends on their respective reliabilities. The weight of the likelihood is expected to be smaller early (when pursuit is largely anticipatory) and is expected to be smaller for the noisier RDKs.

The σ_s and bias parameters of the model were estimated by maximizing the likelihood of the data for each trial n at each time interval t according to the following expression:

$$L\left(\sigma_{\mathrm{s}}, bias|\left\{\theta_{\mathrm{s,t,n}}\right\}_{n=1}^{N}\right) = \prod_{n=1}^{n} \frac{1}{\sqrt{2\pi}\sigma} \times \exp \frac{-[\theta_{\mathrm{t,n}}(\sigma_{\mathrm{s,t,n}}, bias) - \theta_{\mathrm{s,n}}]}{2\sigma^2}$$

Equation 6

where $\sigma = \sqrt{\frac{\sum_{n=1}^{N}(\theta_{\mathrm{t,n}}(\sigma_{\mathrm{s,t,n}}, bias) - \theta_{\mathrm{s,n}})^2}{N-1}}$, $\theta_{\mathrm{s,t,n}}$ is the observed pursuit direction on trial n and at time t, $\theta_{\mathrm{t,n}}(\sigma_{(\mathrm{s,t,n})}$,bias) is the predicted pursuit direction at the given time interval and estimated parameters, and N is the number of trials. Fits were performed using fminsearch function provided by MATLAB.

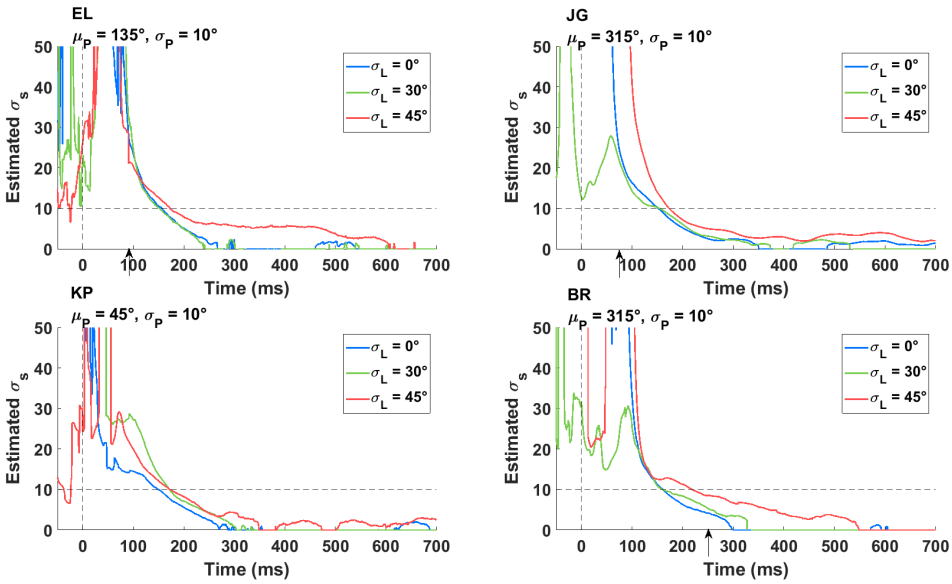

Figure 1.8 A-D: Fit of σ_s parameter for each of the subjects, computed over the timecourse of the trial. Time = 0 corresponds to the onset of stimulus motion. The horizontal line indicates the standard deviation of the prior, σ_P.

Figure 1.8 shows the estimates of σ_s over time for different levels of σ_L. Although anticipatory time intervals are included, σ_s is only meaningful when time > 100 ms following the motion onset time. The results conform to the predictions described above in that the estimated values of σ_s decreased over time and were generally larger for the noisiest motion (σ_L = 45°). The estimate of σ_s decreased at a slower rate and reached values close to 0 later when σ_L was highest (45°). Estimates of σ_s reached values of zero for the clear (σ_L = 0°) or moderately noisy (σ_L = 30°) RDKs by about 300 ms, indicating near total reliance on the likelihood. Estimates of σ_s for the noisiest likelihood remained above zero as late as 600 ms after the onset of target motion. One subject (KP) performed differently in that KP showed smaller differences in σ_s as a function of the noise of the likelihood. This suggests that the internal noise of KP's pursuit system might be higher than that of the other three subjects.

Note that σ_s often takes on values close to 0. There cannot possibly be 0 uncertainty in the sensory likelihood. Thus, the parameter σ_s can be viewed as depending on the uncertainty in the stimulus (which depends on both σ_L and on time relative to motion onset). The parameter σ_s serves to control the relative weight assigned to prior and likelihood (Yin et al., 2019). In other words, a value of σ_s close to 0 will occur when the relative weight assigned to the likelihood is very low in comparison to the prior during the integration of prior and likelihood.

The results (for all except KP) are consistent with the premise of statistically optimal Bayesian cue combination proposed by Kording & Wolpert (2004), at least in a qualitative sense. Optimal cue combination will be subjected to a further test later (Experiment 4) which will focus on the following prediction: If the optimal cue combination model holds and prior and likelihood are combined independently, and if σ_s only relates to uncertainty due to the immediate stimulus, σ_s should only depend on σ_L and not on σ_P. This will be tested later.

3.1.5. Tests of significance

The trend in the estimates of σ_s between levels of σ_L mirror differences in the slopes in Fig 1.7. To determine whether the apparent differences in estimates of the σ_s (and, analogously, the weights on prior and likelihood as determined by the slope in Fig 1.7) for the different levels of σ_L were significant, a likelihood ratio test was performed comparing the results obtained for two levels of σ_L, 30° and 45°. (The results obtained when σ_L= 30° were quite similar to those when σ_L = 0°, thus an additional test involving σ_L = 0° was not performed.) The test compared two nested models. In the constrained

model, the estimated parameters (both σ_s and the bias) for both levels of σ_L, 30° and 45°, were constrained to be the same. In the unconstrained model, σ_s and bias parameters were estimated separately for each value of σ_L. The ratio of the constrained and unconstrained likelihoods is distributed as X^2, with df = 2 (see Cohen et al., 2007, for further description). If the fit of the unconstrained model is significantly better than that of the constrained model, it can be concluded that the noise of the likelihood had significant effects on the directional properties of pursuit.

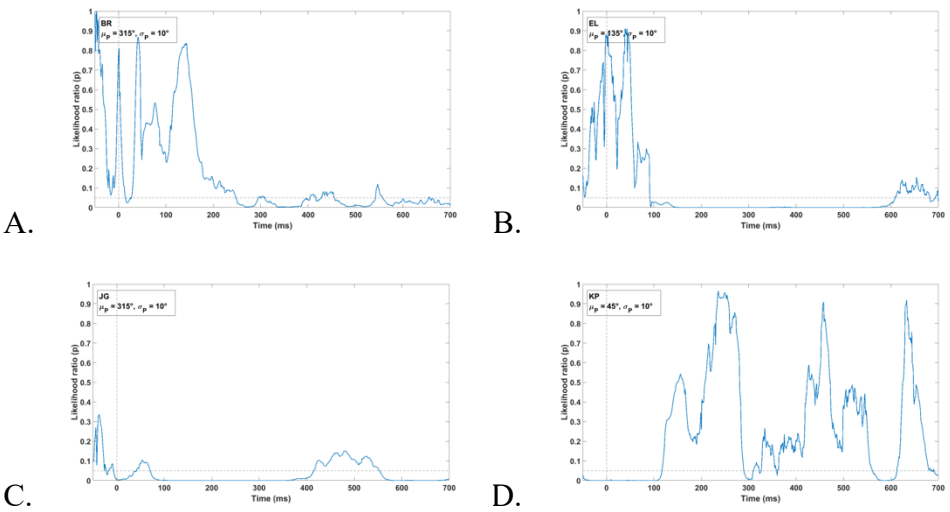

Figure 1.9 A-D: Resulting p value from the likelihood ratio test of the null hypothesis that the constrained model is correct, computed over the timecourse of the trial. Time = 0 corresponds to the onset of stimulus motion. The horizontal line indicates a p value of 0.05.

The p values corresponding to the null hypothesis that the fit of the constrained model is not reliably different from the fit of the unconstrained models are shown in Fig 1.9. For three subjects (EL, JG and BR) p values dropped below .05 about 100-250 ms after the onset of target motion and decreased to values close to zero for most of pursuit. This confirms that effects of the noise of the likelihood were significant. KP does not show significant differences except for a few rare time intervals.

3.1.6. Summary of Experiment 1

The results of Experiment 1 showed a transition in pursuit of RDK's between total reliance on the prior direction of motion to near total reliance on the likelihood (the actual direction of motion) over time. The rate of the transition was slower for the noisiest RDK. Fitting a model of optimal cue combination adapted from Kording & Wolpert (2004) (Eq. 8, Section 1.4.2) showed that the noise of the likelihood affected the estimated weight assigned to the likelihood (captured by parameter σ_s). Specifically, weights decreased over time and were lowest for the noisiest target motions (the latter as predicted by optimal Bayesian cue combination). The weight assigned to the likelihood reached a maximum level ($\sigma_s \sim 0$) only for the clear and moderately noisy RDK. This result indicated that for the noisiest target motion an influence of the prior persisted for at least 500 ms after the onset of target motion.

One subject (KP) showed no differences in pursuit for different levels of RDK noise and all subjects showed little difference between the results for the clear RDKs ($\sigma_L = 0°$) and moderately noisy RDK ($\sigma_L = 30°$). These results suggest that in some cases the RDKs were not sufficiently noisy to overcome internal noise in the motion system (Dakin et al., 2005) or the internal noise of pursuit (Mukherjee et al., 2015). Thus, Experiment 2 was run, which included an even noisier RDK.

3.2. Experiment 2: Noisier likelihood

Experiment 2 tested three levels of σ_L (0, 45 and 60 deg). Five subjects were tested (JG, EL, KP, AP, and WW), including two (AP and WW) who did not run in Experiment 1. For the three subjects who were tested in Experiment 1 data from two

levels of σ_L (0, 45) obtained in Experiment 1 will be included in the report of the results of Experiment 2. Data will consist of 10-17 50-trial blocks for the 45° and for the 60° values of σ_L, interleaved with clear ($\sigma_L = 0$) trials:

Table 3: n trials for each subject in Experiment 2.

Subject	**n trials: $\sigma_L = 45°$**	**n trials: $\sigma_L = 60°$**
JG	17	17
EL	18	13
KP	17	13
WW	14	17
AP	14	11

3.2.1. Preliminary tests to select the mean direction of the prior

For the two subjects who did not participate in Experiment 1, AP and WW, the preliminary tests of pursuit of RDKs in oblique directions were performed to select a value of μ_P. The direction that elicited the fastest eye speeds was selected as the μ_P for the remainder of that subject's experimental sessions. In addition, the value of μ_P was offset from the direction which elicited the fastest pursuit speed by 5-10 degrees to avoid testing a prior with a "salient" direction, such as any of the directions at a 45° angle from the cardinal directions. The direction of μ_P was 35° for AP° and 40° for WW.

A. 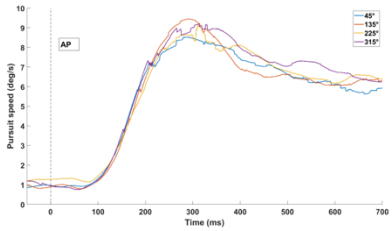

B. 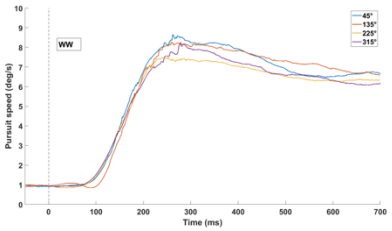

Fig 2.1A and B: Mean pursuit speed over time for the 4 oblique directions (45, 135, 225, 315) for the subjects who did not participate in Experiment 1 (AP and WW). Time = 0 corresponds to the onset of stimulus motion.

3.2.2. Pursuit of RDKs: Speed and direction

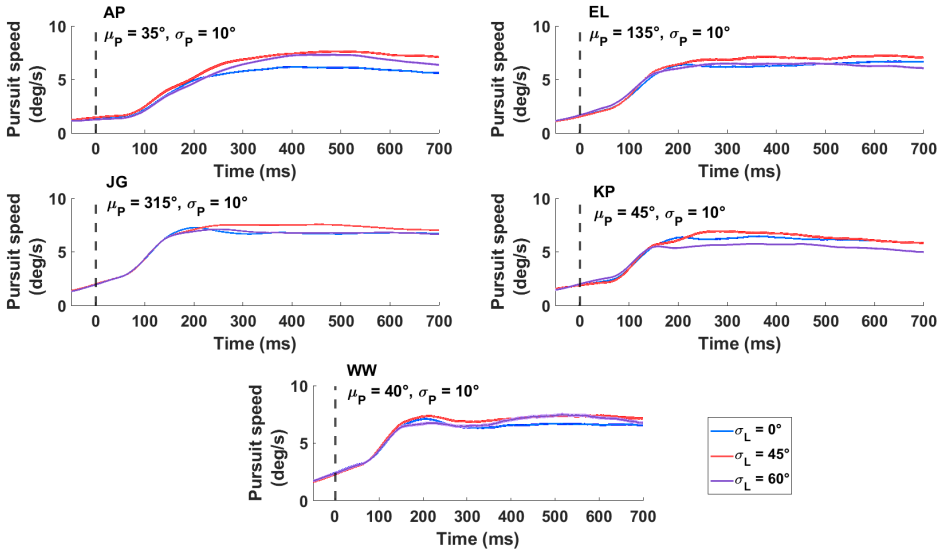

Figure 2.2 A-E: Mean pursuit speed (±SE) over time for each value of σ_L (45, 60) for each of the 5 subjects. Time = 0 ms corresponds to the onset of stimulus motion. Each line corresponds a level of σ_L and the speed of each dot that subject.

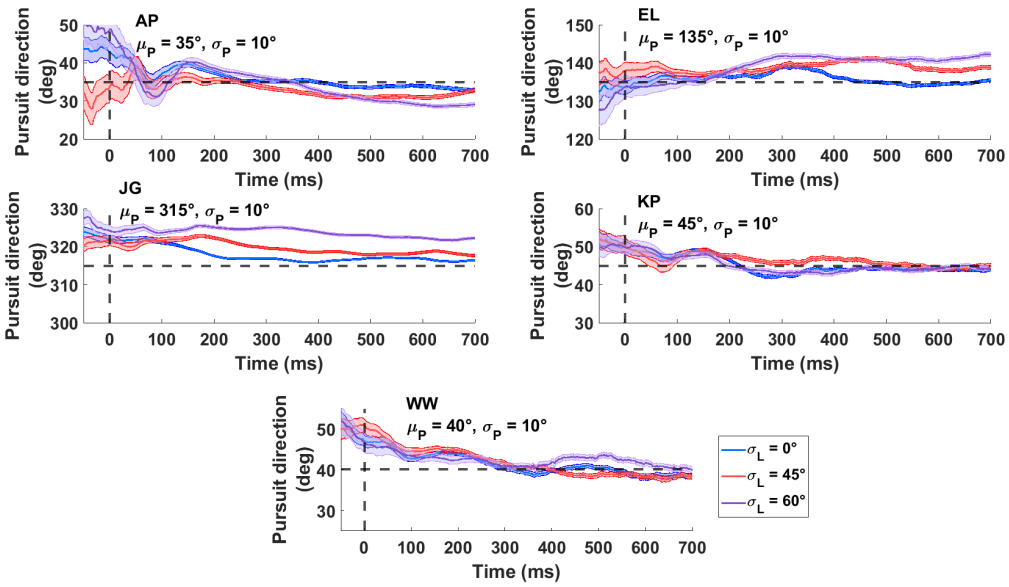

Figure 2.3 A-E: Mean pursuit direction over time for each value of σ_L (45, 60) for each of the 5 subjects. Time = 0 ms corresponds to the onset of stimulus motion. Each line corresponds a level of σ_L and the speed of each dot that subject.

Fig 2.2 shows average eye speed over time for the three values of σ_L, 0°, 45°, and 60°. Recall that the speed of the RDK of each σ_L was varied in order to equate eye speeds across the three levels of σ_L (Section 2.3). Fig 2.2 shows that mean eye speeds were approximately the same across all values of σ_L. This confirms that the choice of dot speed for the different of σ_L was effective in equating the eye speeds.

Anticipatory smooth eye movements were once again seen in Fig 2.2, as shown by the increase in eye speed prior to motion onset and by the mean direction before the motion (Fig 2.3), which was about equal to μ_P. Fig 2.4 shows that SDs were once again similar across different levels of σ_L, though Bartlett's test of homogeneity of variance showed that there were more periods of time with significant differences between the levels of σ_L in some subjects (Fig 2.5).

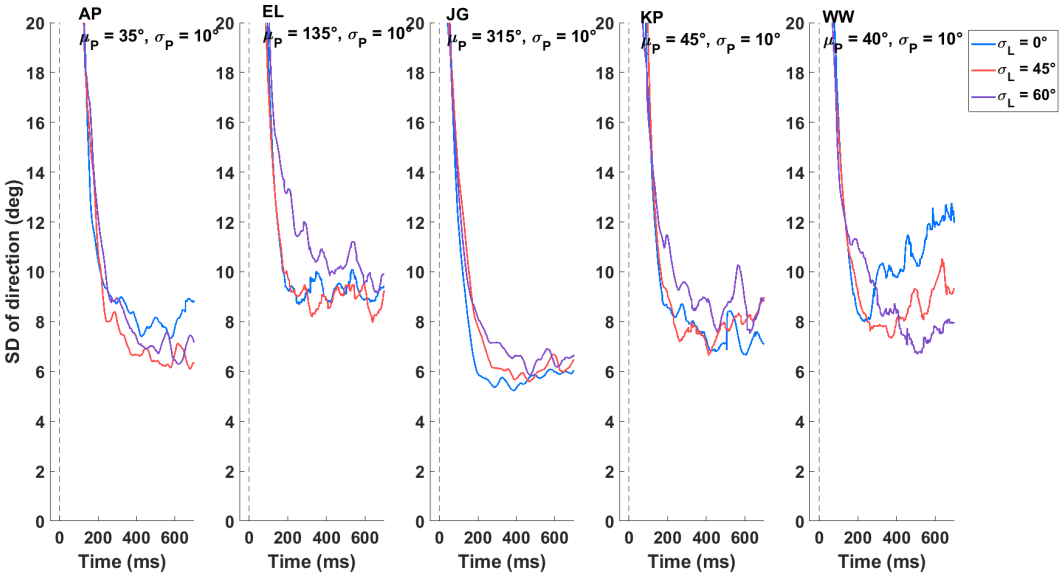

Figure 2.4 A-E. The standard deviation of pursuit direction over time for each value of σ_L for 3 subjects. Time = 0 ms corresponds to the onset of stimulus motion. Each line corresponds to a level of σ_L.

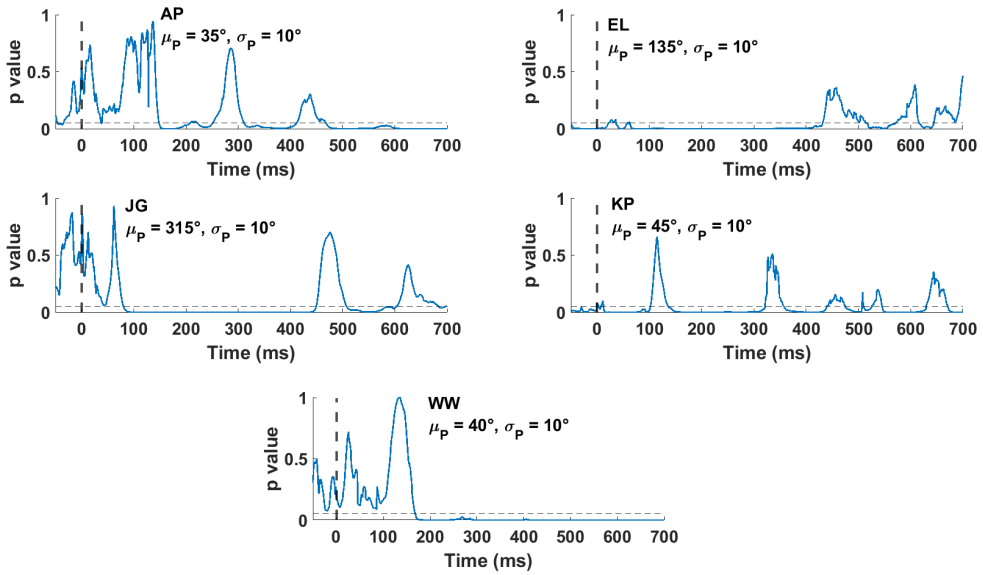

Figure 2.5 A-E: Resulting p value from Bartlett's test of homogeneity of variance, computed for the 3 levels of σ_L over the timecourse of the trial. Time = 0 corresponds to the onset of stimulus motion. The horizontal line indicates a p value of 0.05.

3.2.3. Influence of the prior and likelihood over time

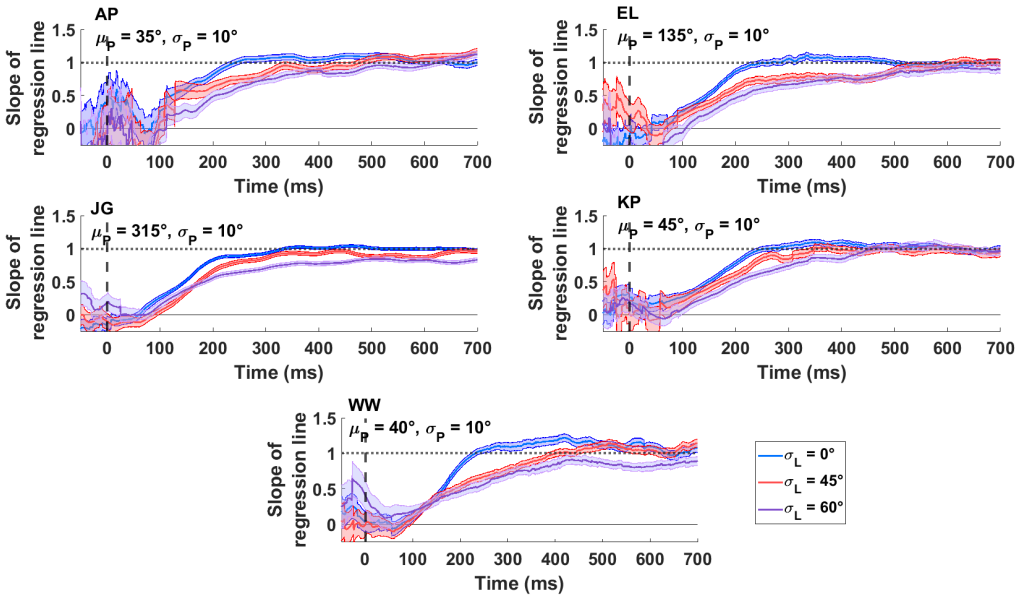

Figure 2.6 A-E: Slope of regression line relating target (μ_L) and eye direction (± SE) on each trial over time. Time = 0 ms corresponds to the onset of stimulus motion. Each line represents a different level of σ_L.

Fig 2.6 shows the slope of the regression line relating target vs eye direction on each trial over time for each of the values of σ_L. The slopes once again gradually increased to values close to 1 over time, showing that pursuit direction increasingly reflected the influence of the direction of the current trial's stimulus motion.

The rate of this increase of the slope of the regression line varied depending on the level of σ_L. When σ_L = 0 deg, slopes reached values near 1 about 200-250 ms after the onset of target motion. When σ_L = 45, slopes reached near 1 later, about 300 ms after target motion onset. The new, noisier value of σ_L, 60, led to slopes of 1 even later, at around 500-600 ms after target motion onset, and in subject JG, never quite reaching 1 in the first 700 ms of the target motion. For all values of σ_L, slopes did not reach 1 until after pursuit reached steady state speeds (see Fig 2.2 for speeds).

Analysis thus far included time intervals up through 700 ms because pursuit was not expected to change appreciably after several hundred ms of constant target motion. Examination of results over the entire duration of RDK motion (1.5 s) showed that for all subjects, the slopes of converged to values close to 1 by around 1 second after the onset of target motion.

3.2.4. Estimating the relative role of prior and likelihood

As in section 3.1.3, Equation 8 outlined in section 1.4.2 was fit to each subject's pursuit data for each of the level of the noise of the stimulus, σ_L, and was computed independently for each time interval in the trial.

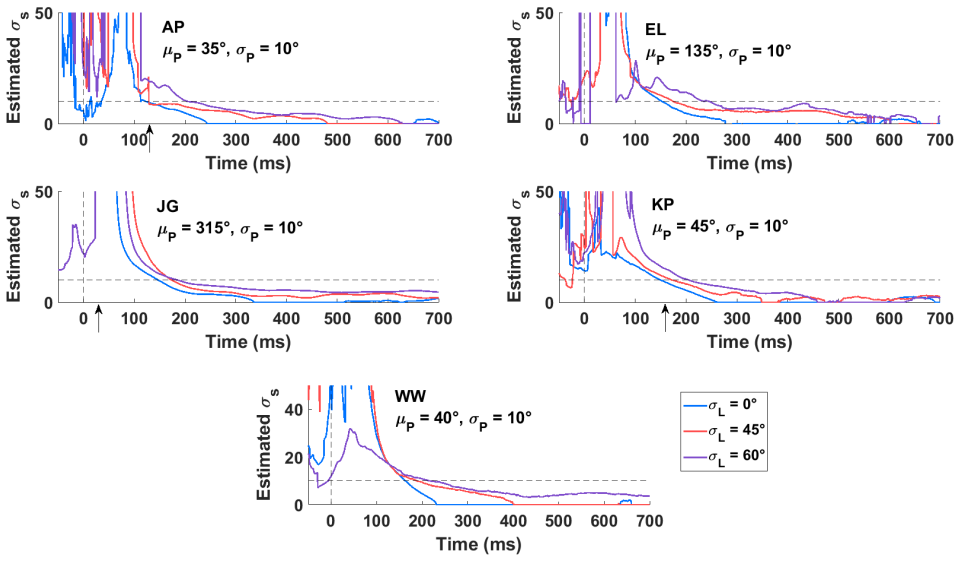

Figure 2.7 A-E: Fit of σ_s parameter for each of the subjects, computed over the timecourse of the trial. Time = 0 corresponds to the onset of stimulus motion. The horizontal line indicates the standard deviation of the prior, σ_P. Arrows indicate the point in the timecourse at which the $\sigma_L = 45°$ and $\sigma_L = 60°$ conditions resulted in a significantly different fit (see Fig 14).

Once again, the estimated value of σ_s (Fig. 2.7) decreased over time reflecting the growing influence of the actual direction of motion of the RDK on that trial. In addition,

as σ_L increased, the estimate of σ_s fell at a slower rate and reached minimum values later in the trial. The likelihood ratio test (see 3.1.5) comparing the fit for $\sigma_L = 45°$ and 60° confirmed that the noise of the RDK, σ_L, had a significant effect on the estimate of σ_s by about 150 ms after the onset of motion. This includes KP, the subject who showed little differences among the less noisy RDK's in Experiment 1.

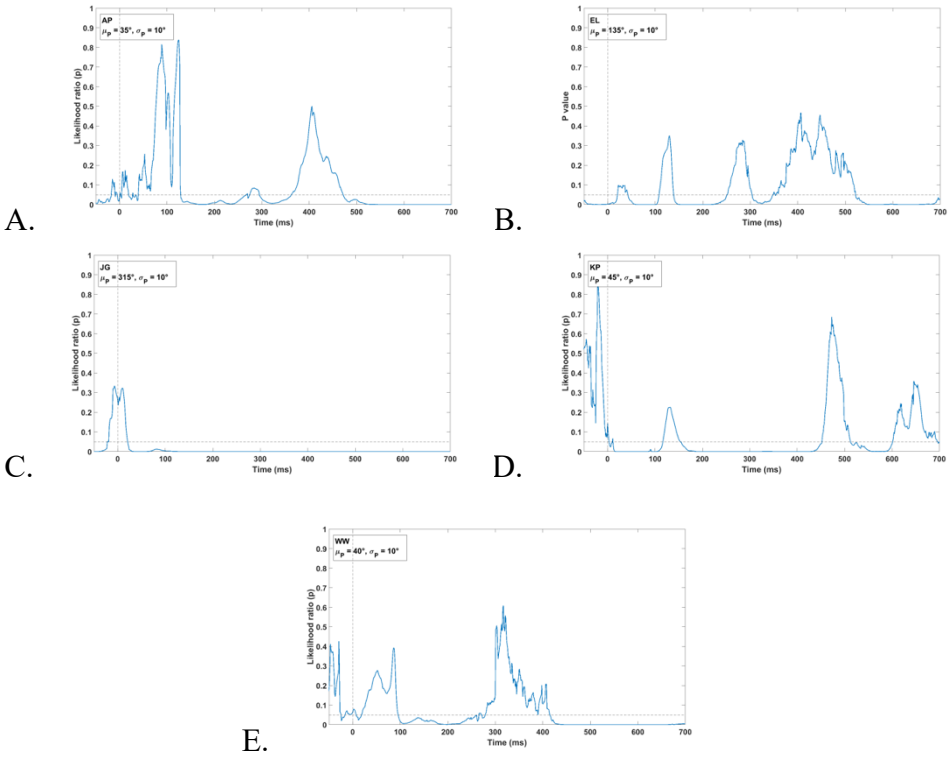

Figure 2.8 A-D: Resulting p value from the likelihood ratio test of the null hypothesis that the constrained model is correct, computed over the timecourse of the trial. Time = 0 corresponds to the onset of stimulus motion. The horizontal line indicates a p value of 0.05.

3.2.5. Summary of Experiment 2

Experiment 2 extended the findings of Experiment 1 to an RDK with a higher level of directional noise. Both Experiments, taken together, support the conclusion that over time pursuit exhibits a transition from total influence on the prior to near total (but

not necessarily complete) influence of the likelihood, and that the relative influence of prior and likelihood depended on their respective reliabilities, as predicted by Bayesian cue combination.

It might be expected that the influence of the prior would have vanished by about 200 ms after the onset of target motion, when pursuit speed reached that of the target. The view that effects of prediction should be limited to intervals before or near the expected onset or change in direction of target motion has been conventional. However, the present results call this conventional view into question. The influence of the prior persisted for longer intervals with the noisier RDKs, as shown by slopes < 1 and by values of the fitted $\sigma_s > 0$ in Figs. 2.7 and 2.8.

3.3. Experiment 3: Variability of pursuit with narrow and uniform priors

The results of Experiments 1 and 2 showed that an increase in the directional noise of the RDK (σ_L) was associated with a greater influence of the prior both during the early portions of pursuit and extending to later, steady state pursuit. Greater directional noise of the target motion might also be expected to lead to greater directional variability of pursuit, but this was not observed. The directional variability (SD of direction) was about the same for all levels of RDK noise (Figs. 1.4, 1.5, 2.4 and 2.5). One exception was WW in Experiment 2, who showed larger SDs for the σ_L of 60 deg.

Experiment 3 examined how the directional variability of pursuit varies with the directional noise of the stimulus (σ_L) with maximal uncertainty about target direction by testing a prior that was uniform across all directions (0° - 360°).

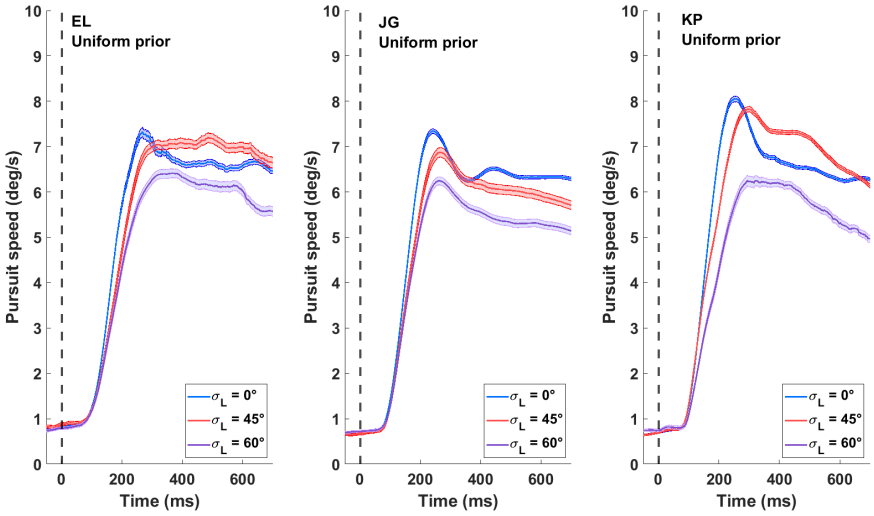

Figure 3.1 A-C: Mean pursuit speed (±SE) over time for each value of σ_L for each of the 3 subjects who participated in Experiment 3. Time = 0 ms corresponds to the onset of stimulus motion. Each line corresponds to a level of σ_L.

Although this section is concerned mainly with directional variability with the uniform prior, average eye speeds were also examined. Fig. 3.1 shows the average speed of pursuit over time with the uniform prior for each subject and level of σ_L. ASEMs were absent, as expected, due to the extremely high directional uncertainty. Pursuit speed increased over time and reached steady state at about 200 ms. Average eye speeds early in pursuit were slightly slower than in Experiments 1 and 2, indicating that the greater directional uncertainty was reflected in pursuit speed. Average speed was also slower for the noisier RDKs, indicating that the "speed scaling" (Section 2.1.c.) did not hold under higher levels of directional uncertainty.

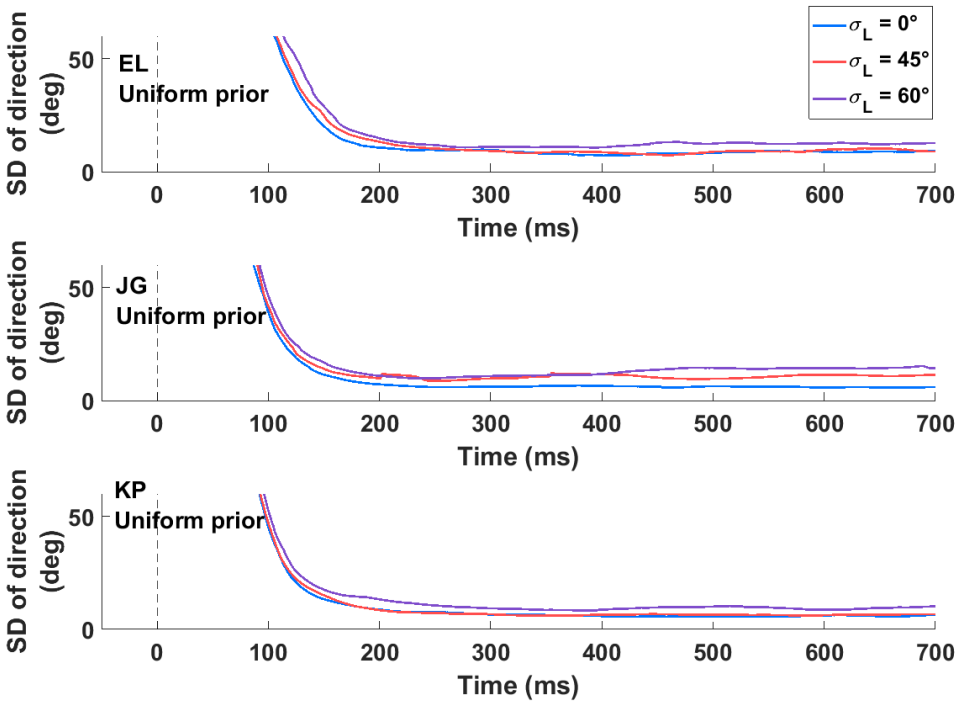

Figure 3.2 A-E: The standard deviation of pursuit direction over time for each value of σ_L for subjects participating in Experiment 2. Time = 0 ms corresponds to the onset of stimulus motion. Each line corresponds to a level of σ_L.

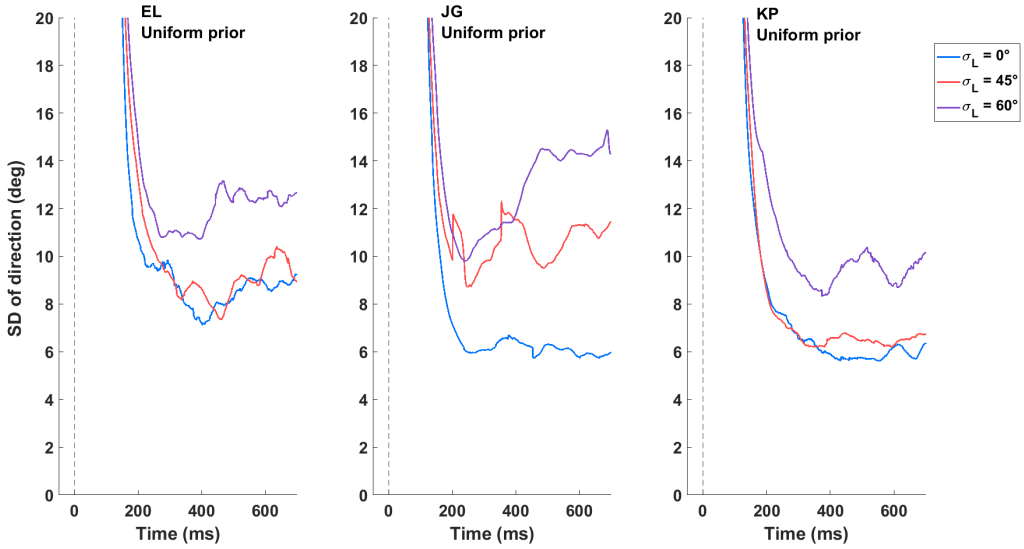

Figure 3.3 A-E: The standard deviation of pursuit direction over time for each value of σ_L for subjects participating in Experiment 2, viewed at a finer scale to emphasize differences in SD between levels of σ_L. Time = 0 ms corresponds to the onset of stimulus motion. Each line corresponds to a level of σ_L.

The standard deviation of the direction of pursuit was computed for each level of σ_L over time (Fig 3.2 and 3.3). The standard deviation was calculated by once again subtracting the mean direction on the current trial (μ_L) from the observed direction of pursuit, leading to a distribution of "direction errors" with a mean of 0. SDs of the resulting distribution were calculated using the CircStat MATLAB package (Berens, 2009) for each level of σ_L.

In contrast to the findings of Experiment 1 and to a greater extent than in experiment 2, Experiment 3 showed an effect of σ_L on the directional variability of pursuit when the prior was more variable (uniform). The difference in directional variability was confirmed by Bartlett's test for homogeneity of variance, which showed a significant difference in the directional variability of pursuit between the 3 levels of σ_L (Fig 3.4).

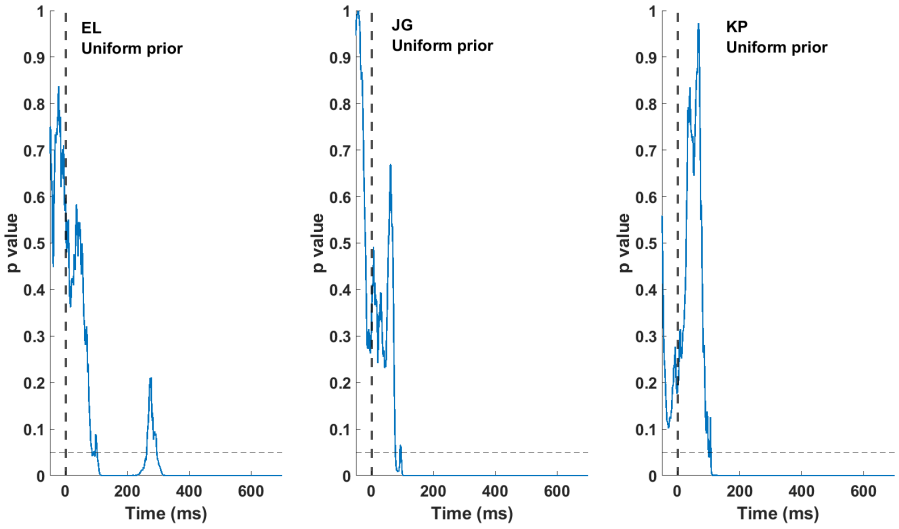

Figure 3.4 A-D: Resulting p value from Bartlett's test of homogeneity of variance, computed for the 3 levels of σ_L over the timecourse of the trial. Time = 0 corresponds to the onset of stimulus motion. The horizontal line indicates a p value of 0.05.

Could this result be due to lower speeds? A faster RDK speed was tested on one subject (JG) and compared with the RDK speed used in the experiment. The eye speed is shown in Fig 3.5, clearly yielding a faster eye speed for the faster RDK. However, as shown in Fig 3.6, the pursuit variability was approximately the same between the two speeds of the RDK, meaning the eye speed by itself was not responsible for the greater directional variability of pursuit found with the uniform prior and the noisier RDKs.

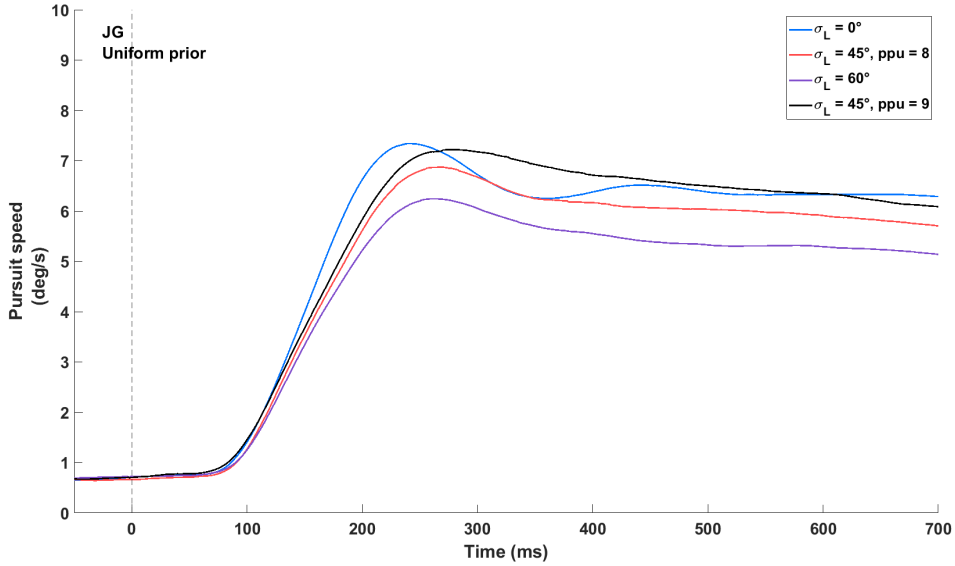

Figure 3.5: The speed of pursuit over time for each value of σ_L for subject JG, for the uniform prior condition. Time = 0 ms corresponds to the onset of stimulus motion. Each line corresponds to a level of σ_L, with the black line representing the set of session sessions with the slightly faster RDK speed.

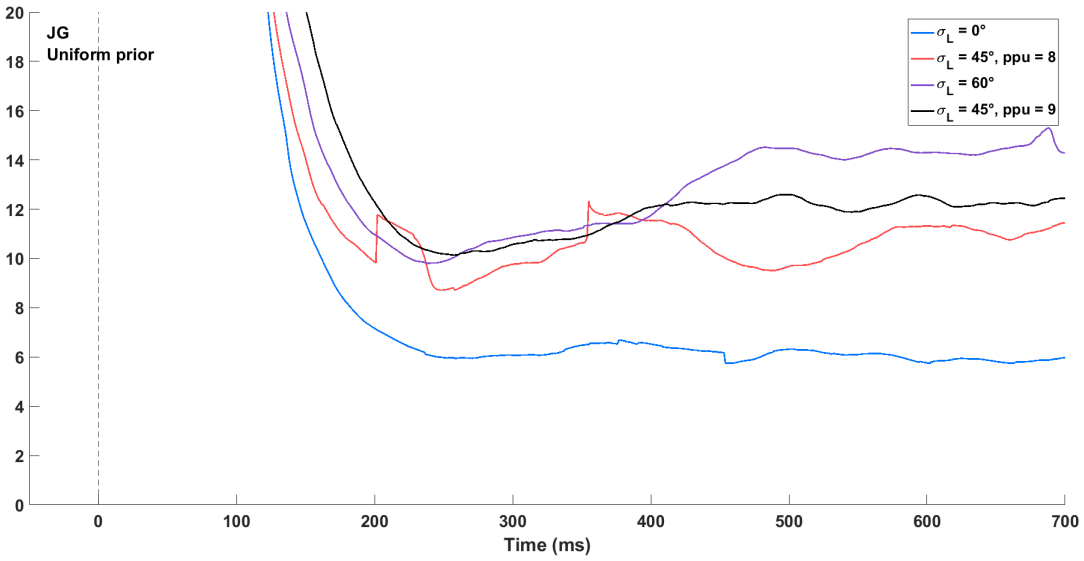

Figure 3.6: The standard deviation of pursuit direction over time for each value of σ_L for subject JG, for the uniform prior condition. Time = 0 ms corresponds to the onset of stimulus motion. Each line corresponds to a level of σ_L, with the black line representing the set of session sessions with the slightly faster RDK speed.

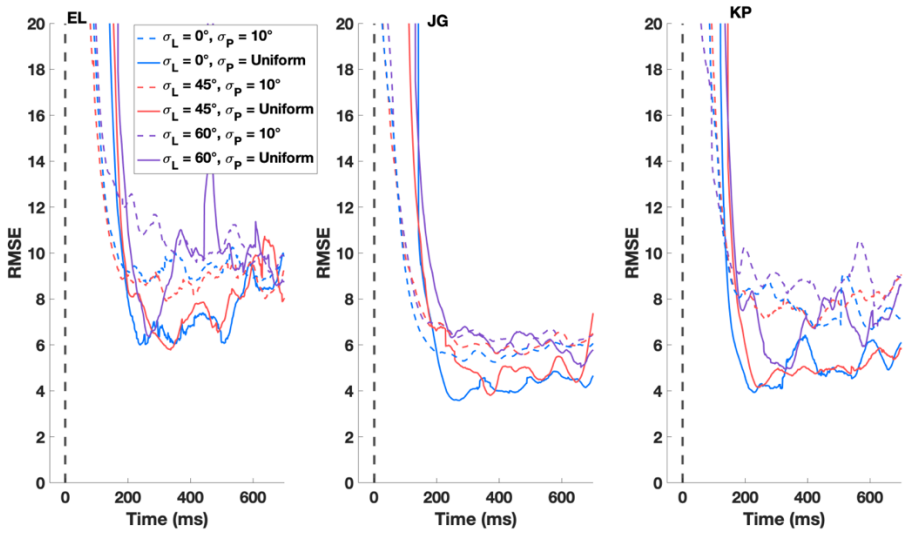

Figure 3.7: The RMS error of pursuit direction around the linear regression line over time for each value of σ_L for the 3 subjects who participated in Experiments 2 and 3. Time = 0 ms corresponds to the onset of stimulus motion. Each line corresponds to a level of σ_L, and σ_P, with the dashed line representing σ_P = 10° and the solid line representing the uniform prior.

Another possible measure of the directional variability of pursuit was plotted by using the root mean squared (RMS) error around the regression lines plotted at each time interval. In order for the uniform prior in Experiment 3 to be compared to the Gaussian prior in Experiment 2, the data analyzed for Experiment 3 was limited to trials where the directions were in the same quadrant as the μ_P used in Experiment 2 ($\mu_P \pm 45°$). This also allowed linear regression to be performed on the circular data. Figure 3.6 shows the RMS error for Experiments 2 and 3. While the overall trend in RMS error as a function of σ_L is not perfectly clear, the RMS error for each value of σ_L are closer together when $\sigma_P = 10°$ rather than when the prior is uniform. These findings suggest that the amount of noise in both the likelihood and prior together affect the variability of pursuit itself.

3.4. Experiment 4: Wider prior

Experiments 1 and 2 showed that with a narrow prior ($\sigma_P = 10°$), changing the variability of the sensory likelihood (σ_L) affected the rate at and extent to which the direction of the likelihood affected the direction of pursuit (Sections 3.1.3 and 3.2.3). While Experiment 3 effectively abolished the prior (the mean of the likelihood was randomly chosen on each trial from a uniform distribution of directions), Experiment 4 used a Gaussian prior that was wider than in Experiments 1 and 2. It is expected that under the assumptions of Bayesian cue combination and Eq 8, the estimates of σ_s for a given time interval and level of σ_L should be reasonably consistent between the two experiments if σ_s is solely reflecting a property of the immediate sensory stimulus. Additionally, if it is found that the estimates of σ_s are consistent between the two levels of σ_P, a predicted result would be that the greater variability of the prior should increase the

reliance on the likelihood earlier in the trial since σ_P is increasing while σ_s remains constant between the two experiments.

Four subjects were tested on a value of σ_P of 45°, rather than the 10° σ_P of Experiments 1 and 2. Two of these subjects, JG and KP, had also run in Experiments 1-3, whereas, so far, HM and VG only ran in Experiment 4. HM and VG are currently being tested with a narrow prior (σ_P = 10°).

3.4.1 Pursuit of RDKs: Speed and direction

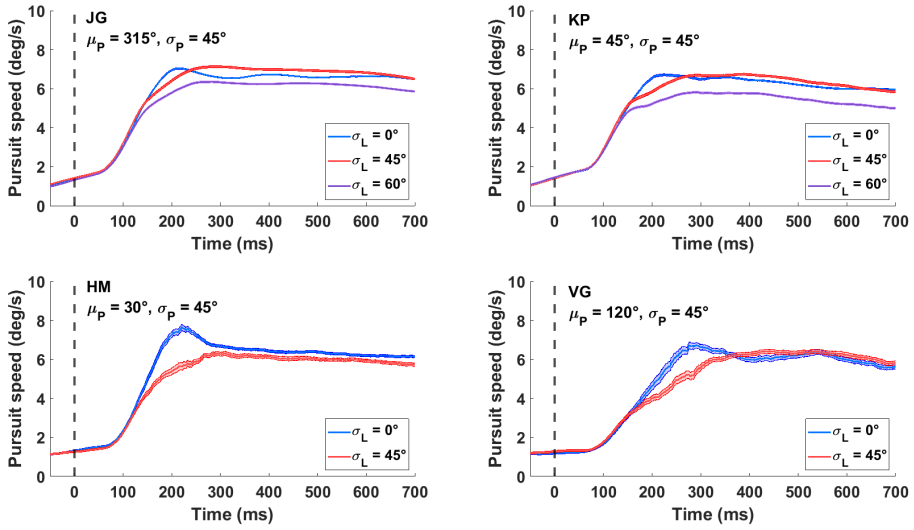

Figure 4.1 A-D: Mean pursuit speed (±SE) over time for each value of σ_L (45 and 60 deg (JG and KP only)) for each of the 4 subjects. Time = 0 ms corresponds to the onset of stimulus motion. Each line corresponds to a level of σ_L.

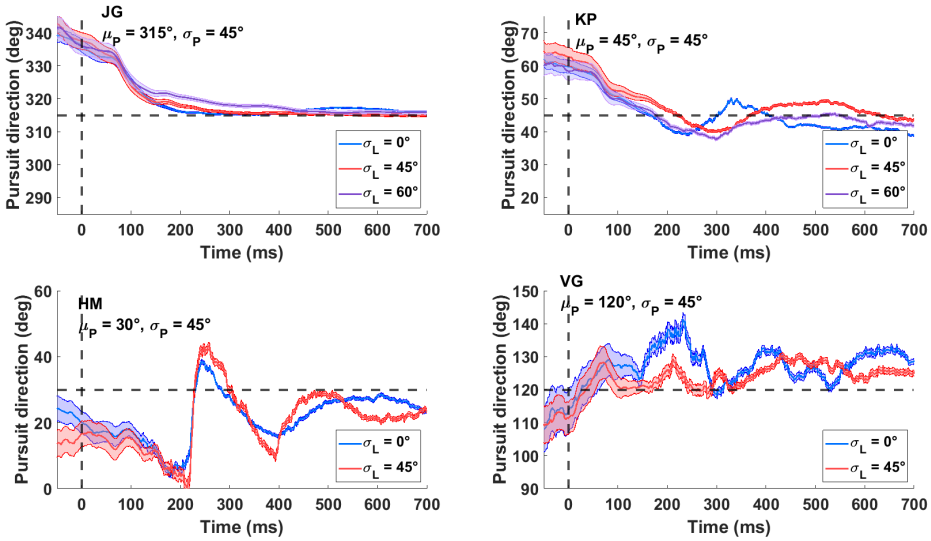

Figure 4.2 A-D: Mean pursuit direction (±SE) over time for each value of σ_L (45 and 60 deg (JG and KP only)) for each of the 4 subjects. Time = 0 ms corresponds to the onset of stimulus motion. Each line corresponds a level of σ_L.

Fig 4.1 shows average eye speed over time for the three values of σ_L, 0°, 45°, and, in 60°. Once again, the speed of the RDK of each σ_L was varied in order to equate eye speeds across the three levels of σ_L (Section 2.3). Fig 4.2 shows that mean eye speeds were approximately the same across all values of σ_L, with some small differences. JG had the fastest pursuit for the σ_L = 45° condition. HM, KP, and VG had faster pursuit in the clear (σ_L = 0°) condition during the ramping up of pursuit speed, but similar steady state speeds in both noise levels (except for HM, who had slightly faster steady state speeds).

Anticipatory smooth pursuit was once again seen in Fig 4.1, as shown by the increase in eye speed prior to motion onset. However, speed of this anticipatory pursuit was slower than with the narrower (σ_P = 10°) prior, about 1°/sec rather than 2°/s at the time of the onset of target motion, reflecting the greater uncertainty about direction.

Furthermore, the average pursuit direction at the onset of motion was further from μ_P for subjects JG and KP than with the narrower prior.

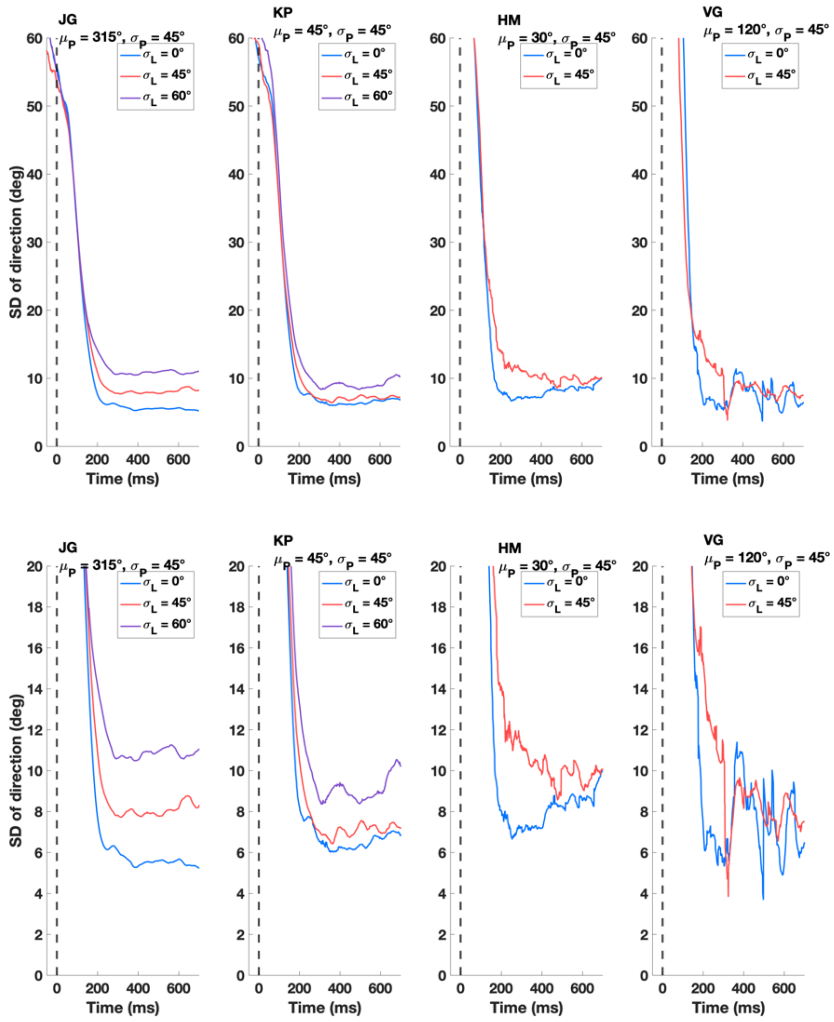

Figure 4.3 A-D: Standard deviation of pursuit direction over time for each value of σ_L (45, 60 (JG only)) for each of the 4 subjects. Time = 0 ms corresponds to the onset of stimulus motion. Each line corresponds a level of σ_L. The bottom plot shows a finer view of the data to emphasize differences in SD between levels of σ_L.

Fig 4.3 shows, as expected, that the standard deviation of the direction of pursuit decreased over time, reaching lowest levels about 200 ms after the onset of target motion. There was an effect of σ_L on directional variability, with the noisier RDKs resulting in more directional variability of pursuit. For 3 subjects, Bartlett's test of homogeneity of

variance showed a significant difference in the directional variability of pursuit between the 3 levels of σ_L through most of the timecourse of the trial for all subjects except VG (Fig 4.4). Additionally, for subjects JG and KP (who were tested in Experiments 1 and 2) pursuit direction was more variable at the onset of target motion than with the narrower prior.

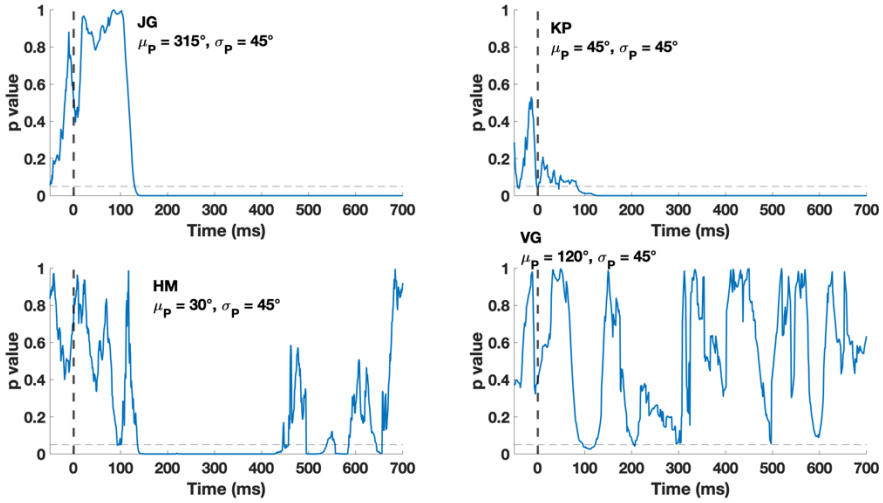

Figure 4.4 A-D: Resulting p value from Bartlett's test of homogeneity of variance, computed for the 3 levels of σ_L over the timecourse of the trial. Time = 0 corresponds to the onset of stimulus motion. The horizontal line indicates a p value of 0.05.

3.4.2. Influence of the prior and likelihood over time

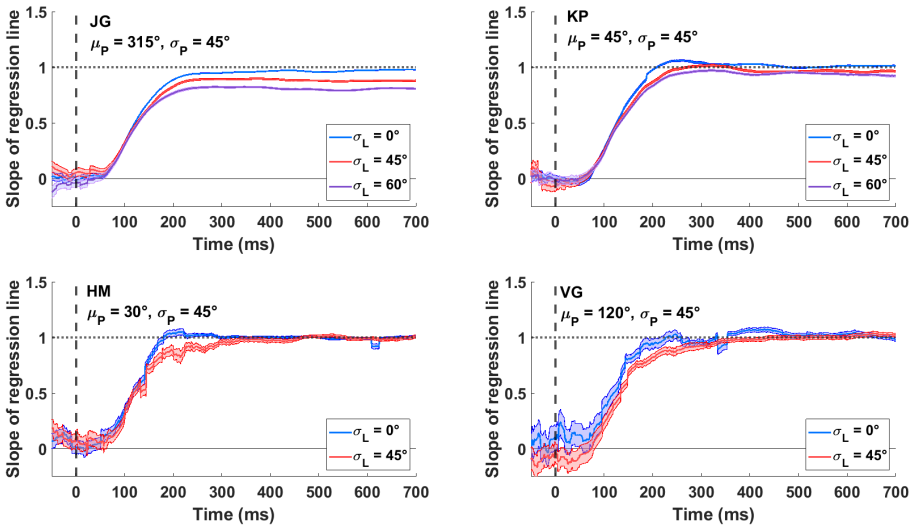

Figure 4.5 A-D: Slope of regression line relating target (μ_L) and eye direction (± SE) on each trial over time. Time = 0 ms corresponds to the onset of stimulus motion. Each line represents a different level of σ_L.

Fig 4.5 shows the slope of the regression line relating target vs eye direction on each trial over time for each of the values of σ_L. The slopes once again gradually increased to values close to 1 over time, showing that pursuit direction increasingly reflected the influence of the direction of the current trial's stimulus motion. Again, there was an influence of σ_L on the slope over time. However, compared to the results from the narrower (σ_P = 10°) prior, the slopes appear to reach near 1 earlier with the wider prior (~40 ms difference) than when the prior was narrow. (See Fig 4.6 and 4.7). This result is consistent with the model of Bayesian cue combination in that adding uncertainty to the prior should lead to a greater influence of the likelihood, particularly early in pursuit, before the influence of the likelihood began to dominate.

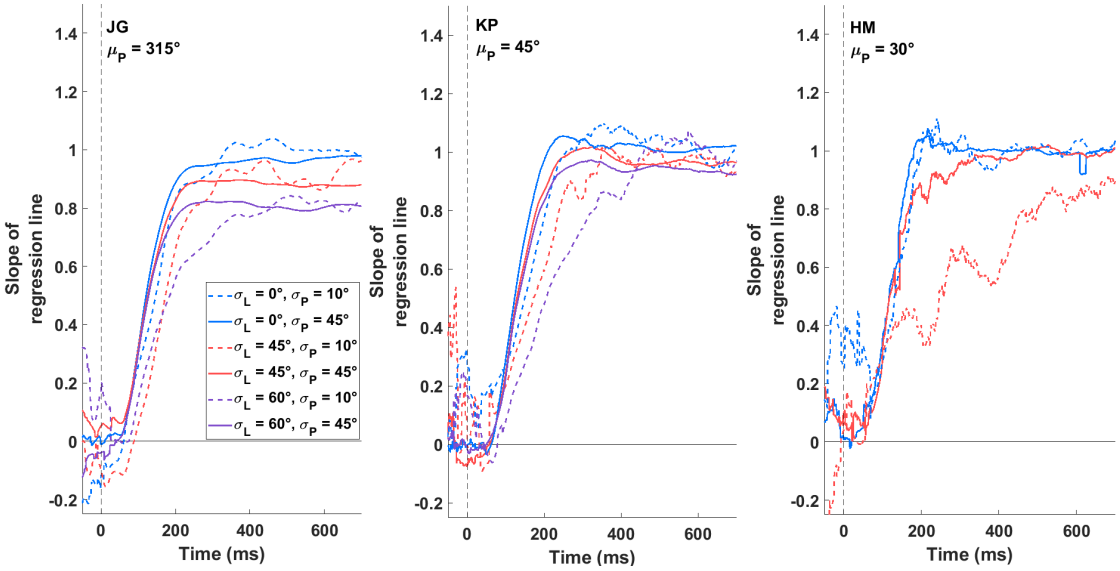

Figure 4.6 A-C: Slope of regression line relating target (μ_L) and eye direction (± SE) on each trial over time. Time = 0 ms corresponds to the onset of stimulus motion. Each line represents a different level of σ_L, with the solid line representing the data from the wider prior ($\sigma_P = 45°$) and the dashed line representing the data from the narrow prior ($\sigma_P = 10°$) from Experiment 2.

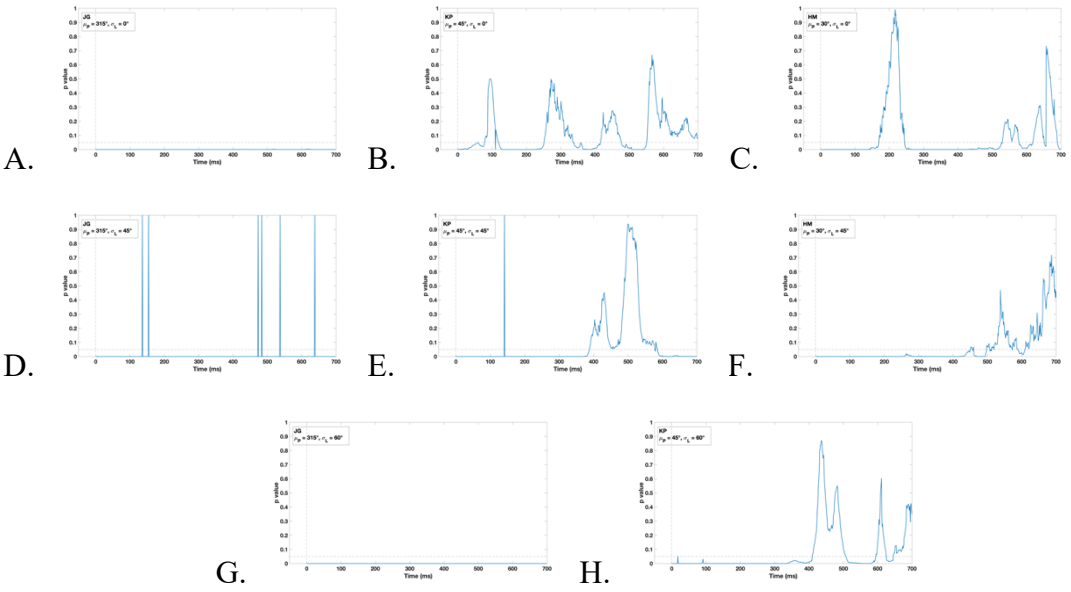

Figure 4.7 A-H: Resulting p value from the likelihood ratio test (between the narrow, $\sigma_P = 10°$, and wide, $\sigma_P = 45°$, priors from Experiments 2 and 4 respectively) of the null hypothesis that the constrained model is correct, computed over the timecourse of the trial for each subject and level of σ_L. Time = 0 corresponds to the onset of stimulus motion. The horizontal line indicates a p value of 0.05.

To attempt to quantify the differences in the progression of slope over time between the narrow prior ($\sigma_P = 10°$) of Experiment 2 and wide prior ($\sigma_P = 45°$) of Experiment 4, a likelihood ratio test was performed comparing the results obtained for two levels of σ_P for the 3 subjects who participated in both levels of σ_P. While subjects JG and KP participated in both Experiments 2 and 4, HM did not participate in Experiment 2, so they were run on a few sessions of the $\sigma_L = 45°$ condition for comparison. Similarly to the likelihood ratio test comparing estimates of σ_s between the levels of σ_L, this test compared two nested models. In the constrained model, the estimated parameters (both σ_s and the bias) for both levels of σ_P, 10° and 45°, were constrained to be the same. In the unconstrained model, σ_s and bias parameters were estimated separately for each value of σ_P. The ratio of the constrained and unconstrained likelihoods is distributed as X^2, with df = 2 (see Cohen et al., 2007). If the fit of the unconstrained model is significantly better than that of the constrained model, it can be concluded that the noise of the prior had significant effects on the directional properties of pursuit (in the slope of the regression line).

Fig 4.7 shows that the results of the likelihood ratio test indicate a significant effect of σ_P on the slope through most of the time for all 3 subjects, with the exception of the clear ($\sigma_L = 0°$) condition for subject KP.

3.4.3. Estimating the relative role of prior and likelihood

As in Experiments 1 and 2, the model (Eq 8) was fit to the pursuit directions for each level of the noise of the likelihood (σ_L). The estimates of σ_s for Experiment 5 are

shown in Fig 4.8. σ_s decreased to 0 at a faster rate for the clear ($\sigma_L = 0°$) than the noisy ($\sigma_L = 45°$) RDK.

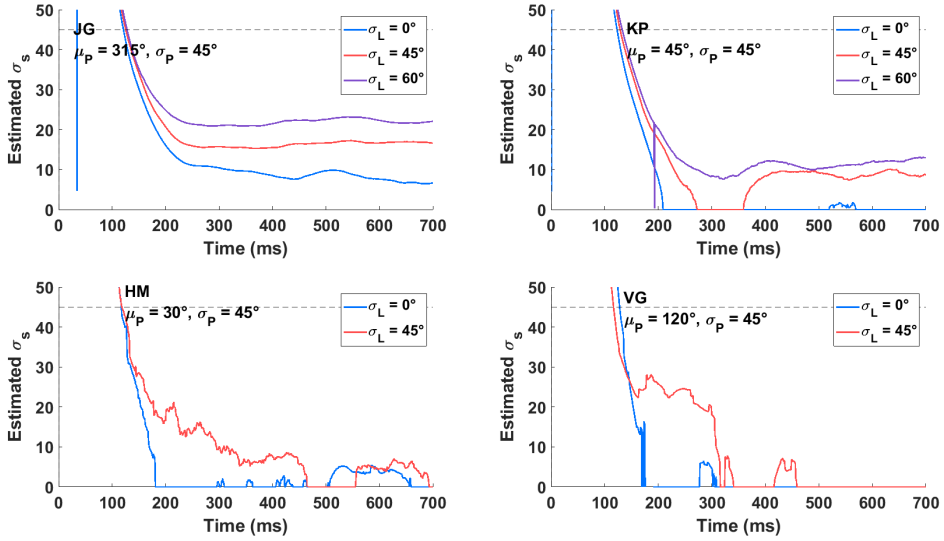

Figure 4.8 A-C: Fit of σ_s parameter for each of the subjects in Experiment 4, computed over the timecourse of the trial. Time = 0 corresponds to the onset of stimulus motion. The horizontal line indicates the standard deviation of the prior, σ_P.

With the exception of the clear condition, the σ_s estimates for all subjects are different between Experiments 2 ($\sigma_P = 10°$) and 4 ($\sigma_P = 45°$). Specifically, the estimates of σ_s when $\sigma_L = 45°$ are about 10-15° with the wider prior during steady state pursuit, greater than the 5-10° found with the narrow prior. This incompatibility of the estimates of σ_s between the levels of σ_P do not agree with the predictions under the model (Eq. 8), which would predict a similar estimate of σ_s across the different values of the prior uncertainty if the prior and likelihood contributed independently. The higher estimated σ_s with the wider prior would tend to overestimate the weight assigned to the prior, perhaps indicating that the variability of the wider prior was underestimated.

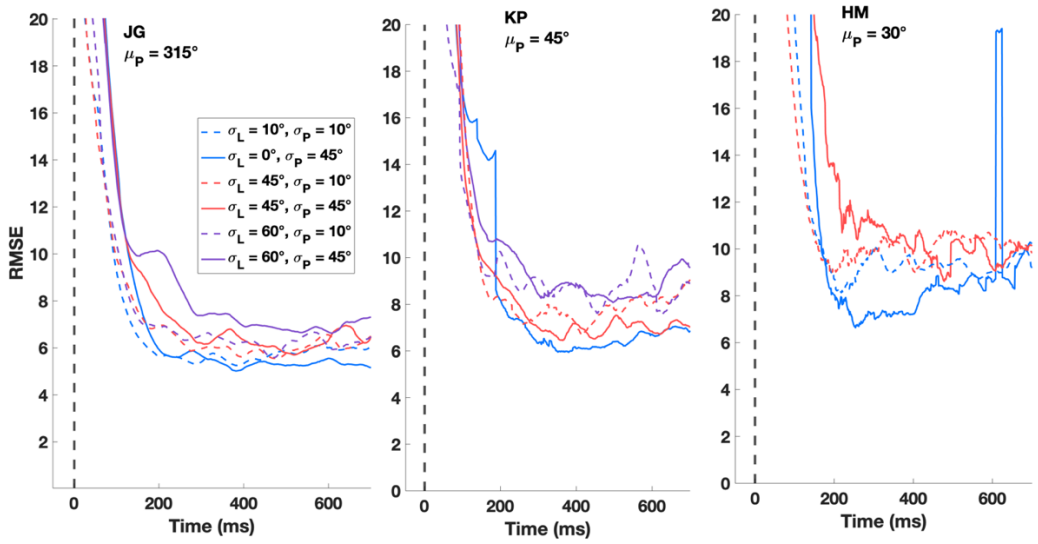

Figure 4.9 A-C: The RMS error of pursuit direction around the linear regression line over time for each value of σ_L for the 3 subjects who participated in Experiments 2 and 4 (with the exception of HM, who did not participate in Experiment 2 but ran in some test sessions with the $\sigma_P = 10°$ prior). Time = 0 ms corresponds to the onset of stimulus motion. Each line corresponds to a level of σ_L, and σ_P, with the dashed line representing $\sigma_P = 10°$ and the solid line representing $\sigma_P = 45°$.

As with the uniform prior (Experiment 3), the RMS error was computed around the linear regression line over time. Figure 4.9 shows the RMS error for subjects who participated in Experiment 4 and Experiment 2 (HM participated in several sessions of the $\sigma_P = 10°$ prior for comparison). To reduce any differences in pursuit which may appear when targets move in different quadrants from the one analyzed in Experiment 2, the data for Experiment 4 was restricted so that only the target directions in the same quadrant of the prior were included in the analysis ($\mu_P \pm 45°$). As with the uniform prior in Fig 3.7, the effect of the level of σ_L on RMS error appears to be greater when the prior was more variable.

3.5. Experiment 5: Effect of RDK speed

As noted earlier, stimulus speed was varied across levels of σ_L to equate speeds when pursuit speeds reached steady state. This process was not perfect, and thus there were occasionally small discrepancies between the eye speeds across the different levels of σ_L. To determine whether small differences in eye speed affect the relative role of prior and likelihood, 3 subjects (JG, EL, and KP) were tested on two stimulus speeds using clear RDKs.

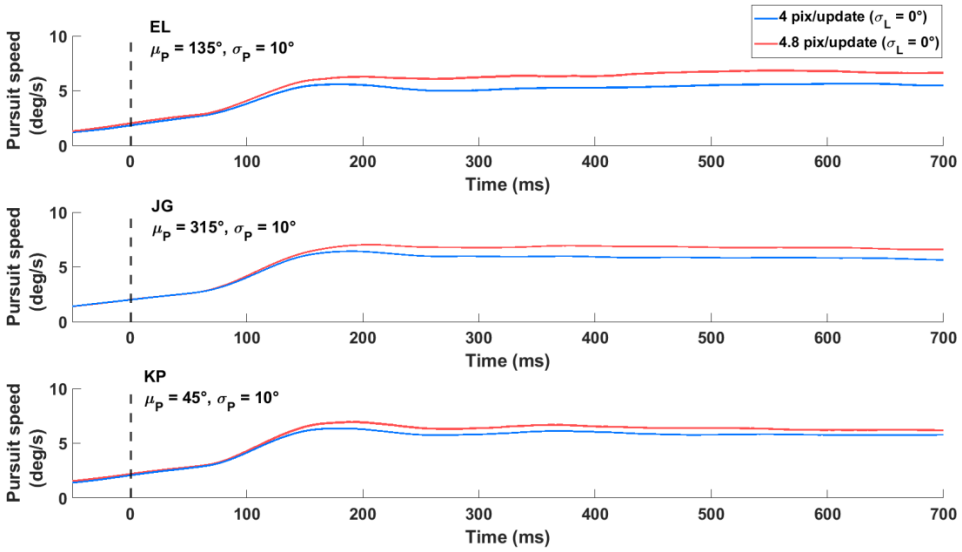

Figure 5.1 A-C: Mean pursuit speed (±SE) over time for speed of the RDK dots (4.0 or 4.8 pixels/frame), for each of the 3 subjects. Time = 0 ms corresponds to the onset of stimulus motion.

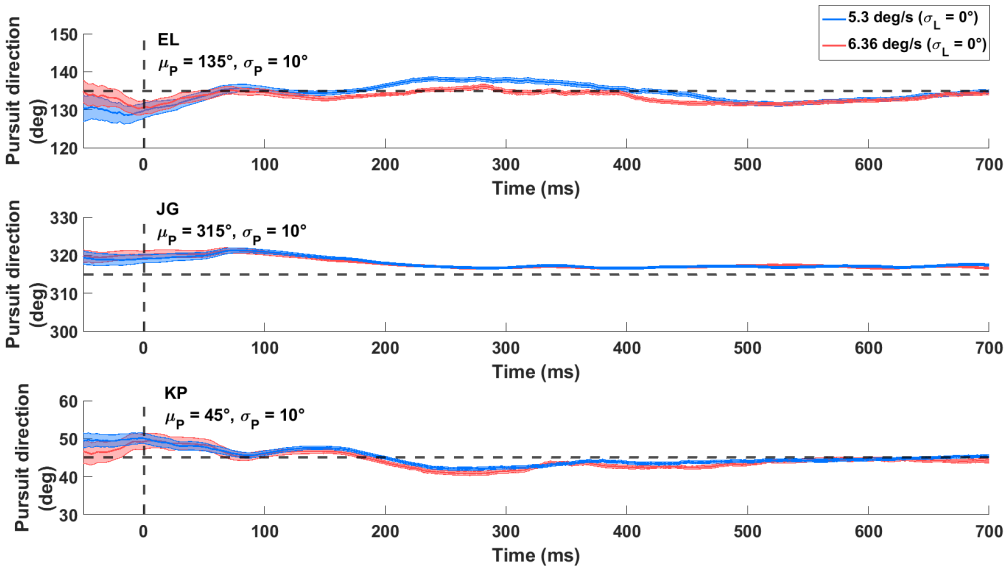

Figure 5.2 A-C: Mean pursuit direction (±SE) over time for speed of the RDK dots (4.0 or 4.8 pixels/frame), for each of the 3 subjects. Time = 0 ms corresponds to the onset of stimulus motion.

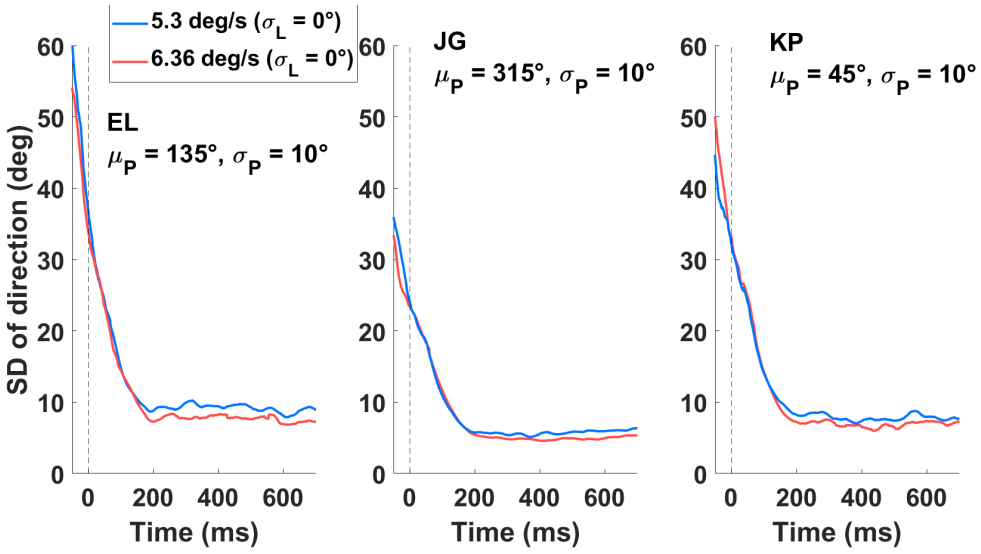

Figure 5.3 A-D: Standard deviation of pursuit direction over time for speed of the RDK dots (4.0 or 4.8 pixels/frame), for each of the 3 subjects. Time = 0 ms corresponds to the onset of stimulus motion. Each line represents a different speed of the RDK.

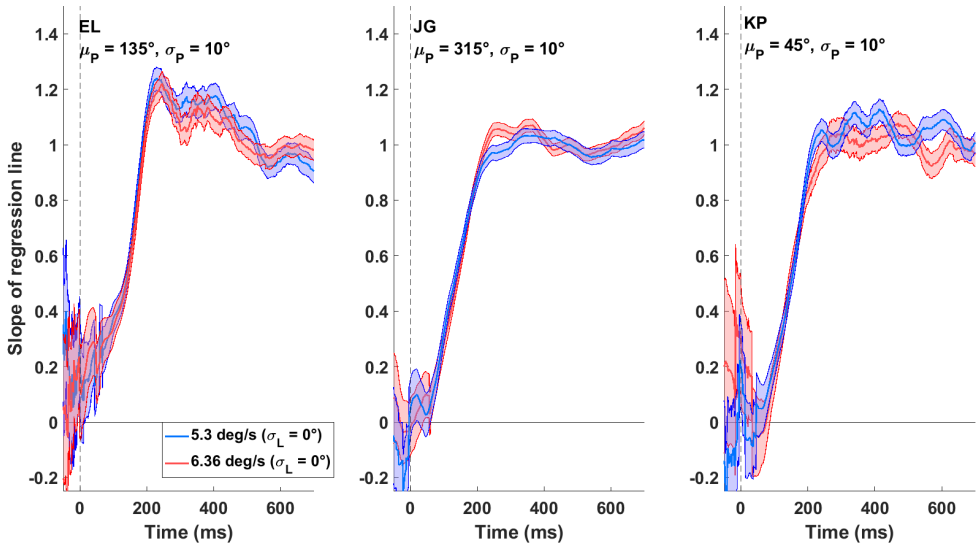

Figure 5.4 A-D: Slope of regression line relating target (μ_L) and eye direction (± SE) on each trial over time. Time = 0 ms corresponds to the onset of stimulus motion. Each line represents a different speed of the RDK.

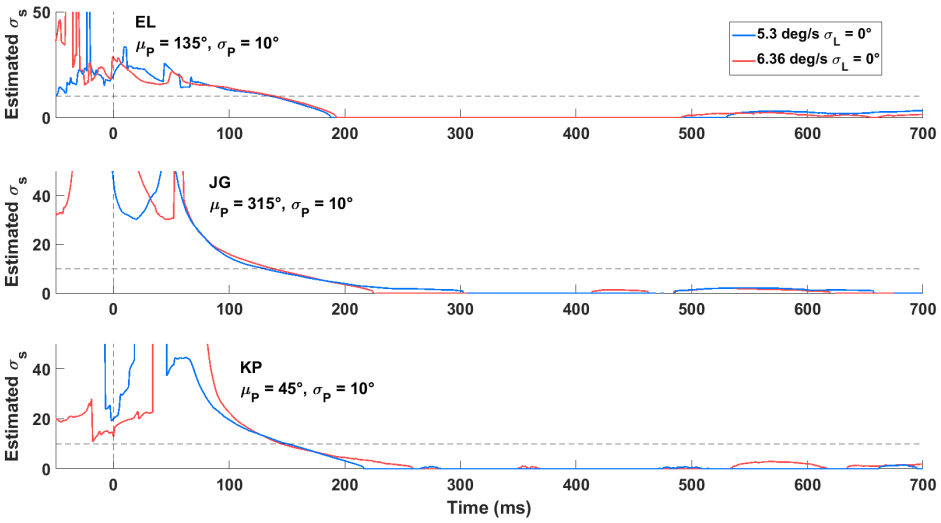

Figure 5.5A-C: Fit of σ_s parameter of the model for each of the subjects, computed over the timecourse of the trial, for the two speeds of the clear condition in Experiment 6. Time = 0 corresponds to the onset of stimulus motion. The horizontal line indicates the standard deviation of the prior, σ_P.

Fig 5.1 shows average pursuit speeds for the two levels of RDK speeds tested. Mean direction over time was not affected by the speed of the target (Fig 5.2). Standard deviations of the direction of pursuit were slightly higher for the slower speeds. The slopes of the regression line relating target vs. eye direction on each trial (Fig 5.4) and the estimated values of σ_s were quite similar for both speeds. Additional data will be collected to verify this result with a wider range of speed and with the noisy RDKs.

3.6. Experiment 6: Perceptual reports

The perceptual reports of the direction of the RDK that were collected at the end of each trial in Experiments 1-5 were mainly used to motivate attention to the displays rather than assess the perceptual evaluation of the mean of the RDK. The interpretation of these reports could have been affected by the sensed position of the eye at the end of the trial, when the eye reached the perimeter of the display.

As outlined in section 2.2.b, a separate experiment was conducted to determine how the noise of the RDK (σ_L) affected perceptual reports. This experiment used a short presentation of the motion stimulus (150 ms) to prevent sustained pursuit.

This experiment also used as a mask consisting of dots moving in a direction chosen from a uniform distribution on each frame presented before and after the critical motion frames to prevent visual persistence of the motion and better control processing duration. Both pre- and post-masks have been used before to limit processing duration (Buhcall & Kowler, 1999). In addition, there was no fixation point in order to minimize cues to relative motion. The clear ($\sigma_L = 0°$) and noisy ($\sigma_L = 45°$ and $60°$) RDKs were tested. Three subjects were tested in the $\sigma_L = 60°$ condition, and 5 were tested in the

clear ($\sigma_L = 0$) and $\sigma_L = 45°$ condition. Note that subject EL often reported that the dots were moving 180° in the opposite direction, perhaps due to some type of wagon wheel illusion. As such, any trials with outlier responses outside of a 90° range from μ_L were left out of the analysis.

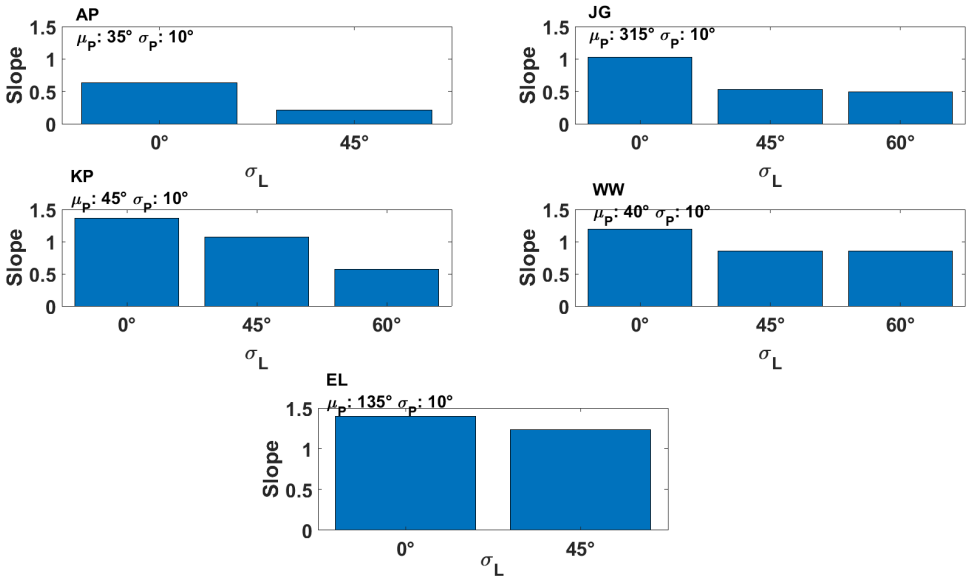

Figure 6.1A-E: Bar graphs depicting the slope of the regression line relating the mean direction of the dots on each trial (μ_L) and the response from the subject at the end of the trial for all 5 subjects and 3 levels of σL.

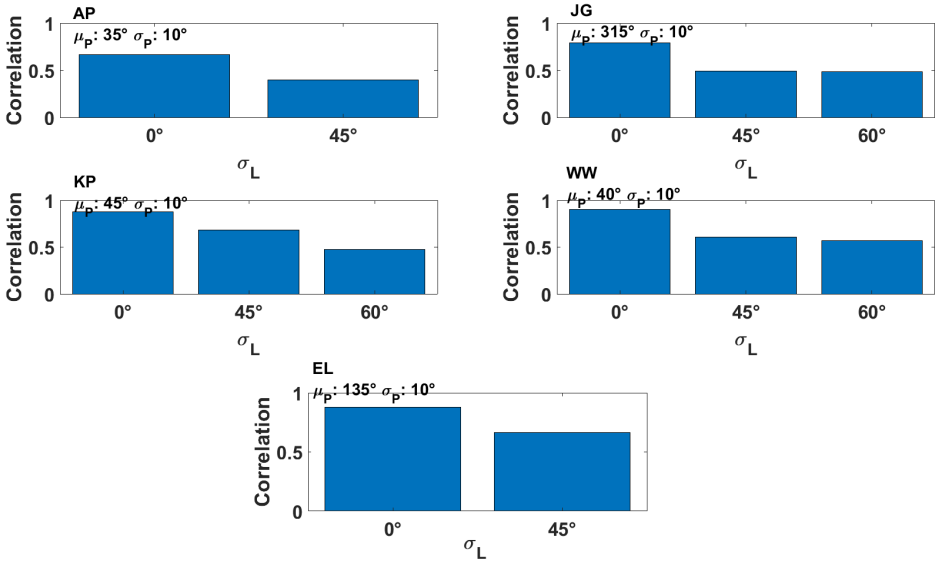

Figure 6.2 A-E: Bar graphs showing the circular correlation between the mean direction of the dots on each trial (μ_L) and the response from the subject at the end of the trial for all 5 subjects and 3 levels of σL.

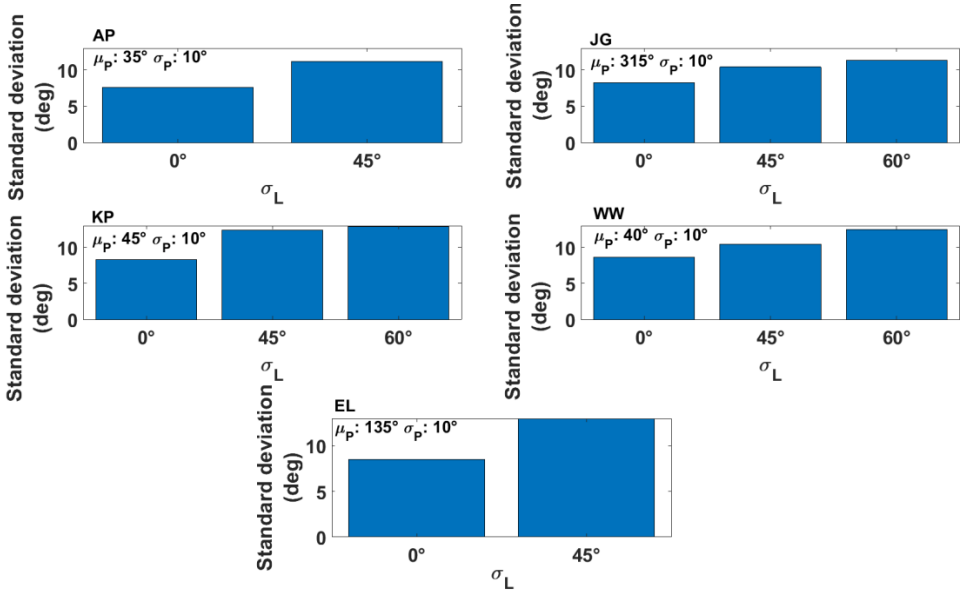

Figure 6.3 A-E: Bar graphs showing the circular standard deviation of subject responses at the end of the trial for all 5 subjects and 3 levels of σ_L.

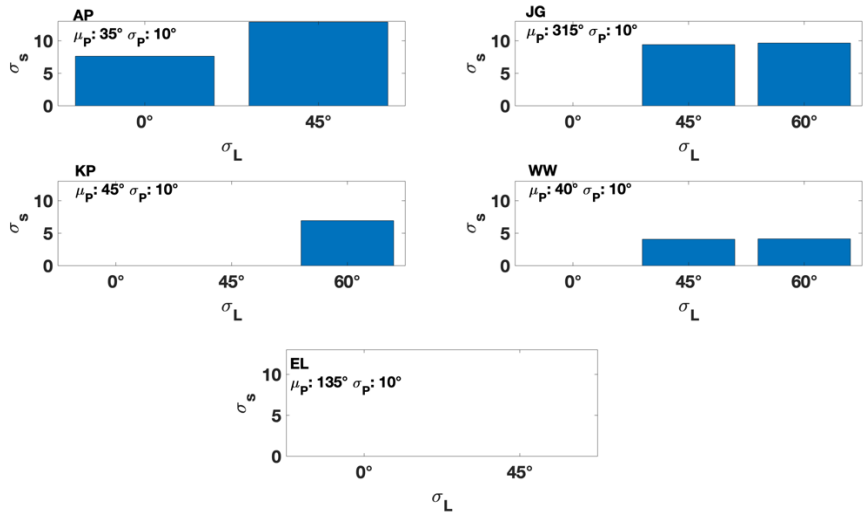

Figure 6.4 A-E: Bar graphs showing the estimated σ_s parameter fit to the Bayesian model for all 5 subjects and 3 levels of σ_L.

Once again, linear regression was used this time to relate the direction of the stimulus motion on each trial (μ_L) with the reports of the perceived direction of motion. Fig 6.1 shows that the slope of the regression line decreased as the directional noise of the RDK (σ_L) increased for all subjects, with some subjects' responses resulting in a slope greater than 1 (meaning the reports tended to be biased away from μ_P the further the value of μ_L on that trial).

The correlation between the stimulus direction (μ_L) and the subjects' responses also decreased, and the standard deviation of the responses around the regression line increased as σ_L increased (Fig 6.3), similar to what was found in pursuit of the wide and uniform priors. The value of the σ_s obtained from fitting the model introduced in Eq. 8 increased as σ_L increased in all subjects except EL (Fig 6.4).

Taken together, the results for the short presentation condition in Experiment 6 show that perception of motion direction may be similar to pursuit in that the influence of the actual direction decreased relative to the prior as directional noise

4. Discussion

4.1. Overview

Since the early days of smooth pursuit research, it has been observed that pursuit anticipates the future target motion. Classical studies as far back as Westheimer (1954) and Dallos & Jones (1963) have shown patterns of predictive pursuit in response to periodic target motion, with the eye moving ahead of a change in direction of the target (Kowler & Steinman, 1979). These findings were later extended beyond simple extrapolation of stimulus motion to reveal that pursuit involves a complex interaction between cognitive and sensory-based inputs. These studies have shown anticipatory smooth eye movements (ASEM) manifesting as not only a bias in pursuit based on previous target motion (Kowler & McKee, 1987; Kowler et al., 1984; Yang & Lisberger, 2012) but also in response to verbal or visual cues (de Hemptinne, Lefèvre, & Missal, 2006; Kowler, 1989, Santos & Kowler, 2017).

While ASEM has been observed in various forms for over 50 years, the role of anticipation has been less understood. Prior work has suggested ASEM could be useful for overcoming processing delays which the system would incur if pursuit only relied on incoming sensory signals. However, the findings of the current study suggest a new, additional role for anticipation: the overcoming of noise in the sensory motion signal or in the motor signal (or both). When sensory inputs were more variable (specifically, random dot kinematograms with high levels of directional noise), the results showed an increased and longer lasting influence of the prior on pursuit, resulting in the eye moving with about the same level of directional variability across the noise levels of the RDK stimulus. When the prior became less reliable, the influence of the immediate motion

appeared earlier in time. In addition, there were suggestions that the directional variability of pursuit was affected more by changes in the directional noise of the stimulus with the less reliable prior. This increased influence of the prior as sensory uncertainty increased, and the increased influence of the likelihood as the uncertainty of the prior is increased, is conventional in processes which are governed by the tenets of Bayesian cue combination, such as a variety of different perceptual judgements or motor behaviors (Kording & Wolpert, 2004).

These new findings reveal insights into the process of integrating anticipation and sensory response in pursuit. While there still appear to be clear stages of mostly anticipation-driven and mostly sensory-driven smooth pursuit, the present study shows evidence for a combination and reweighting of the two signals in proportion to their respective reliabilities in a way that is at least qualitatively consistent with the principles of Bayesian cue combination. This concept of the integration of an extraretinal signal with a sensory signal is not new, with previous models incorporating either a switching mechanism (Barnes & Collins, 2008) or a reliability-weighted sum (Orban de Xivry, 2013), but is tested here more directly by explicit experimental manipulation of the reliability of the retinal and extraretinal components.

4.2. Summary of results and main conclusions

There were a number of main experimental results:

1. The direction of smooth pursuit was affected by the directional variability of both the prior and the likelihood, where prior refers to the distribution of

means of the likelihood across trials, and likelihood refers to the distribution of the direction of the dots on the current trial.

2. When the directional variability of the RDK was higher, the effect of the prior on the direction of pursuit persisted for a longer duration relative to the onset of target motion (Experiments 1 and 2). This was reflected by two results. First, the mean direction of pursuit during the interval from -100 ms to ~100 ms relative to the start of target motion was close to the mean direction of the prior. Second, the slope of the function relating target and pursuit direction reached a value of 1 later in time for noisier levels of the likelihood (greater σ_L). Slopes could require as long as ~600 ms to reach a value close to 1. The more variable the likelihood, the longer it took for slopes to reach a value close to 1.
3. When the directional variability of the prior was higher, the slopes reached a value near 1 earlier (Experiment 4) than with priors with less directional variability (Experiments 1 and 2).
4. The perceptual responses (Experiment 5) showed similar trends as found for pursuit. The slopes of the lines relating target direction and perceptual reports increased as directional variability of the RDK decreased. Also, the variability of the perceptual reports increased with directional variability of the RDK.
5. The extent to which the results conform to the premise of Bayesian cue combination was assessed by fitting by an expression relating prior and likelihood as a function of their respective reliabilities adapted from Kording

& Wolpert (2004). Here, pursuit direction at any point in time was a weighted sum of the mean direction of the prior and the mean direction of the likelihood on a given trial, where the weights were proportional to the reliability of prior and likelihood. Fitting the model required estimating two parameters, the parameter representing the processing noise (σ_s) of the likelihood and a bias parameter. As expected, values of σ_s decreased over time and were higher for noisier likelihoods. However, the estimated value of σ_s was different for different levels of the variability of the prior. This suggests that additional features may need to be added to the model, such as a provision to allow misestimates of the mean or standard deviation of the prior, or non-independence of prior and likelihood.

These results show that basic principles of Bayesian cue combination can apply smooth pursuit eye movements.

4.3. Comparison with previous work

Orban de Xivry et al. (2013) implemented a model of pursuit with two major components, each with a Kalman filter. One component of the model dealt with processing visual input, whereas the other maintained and updated memory about past target motion (where past in their model referred to target motions seen on previous trials). The outputs of both Kalman filters were then statistically combined in proportion to their respective reliabilities. The model was then able to exhibit classical examples of predictive and sensory-driven smooth pursuit without requiring a neural “switch” to take

prediction in or out of the control circuitry (Barnes & Collins, 2008). However, the model was not fit to experimental data, but rather simulated phenomena qualitatively. The model also required many parameters (12) which were estimated statistically or from previous data and examined effects in which the level of uncertainty about target motion was varied by blanking the target briefly during its motion. The current work estimates two parameters and varied uncertainty by manipulating the directional variability of the prior and the motion stimulus directly. The variability of the motion stimulus was manipulated by modifying the spread of the Gaussian distribution defining each signal, a manipulation that has been shown to affect direction discrimination of RDKs (Watamaniuk et al., 1989).

Another recent model of predictive smooth pursuit, Bogadhi et al. (2013) was able to show a dynamic reweighting of retinal and extraretinal signals which combined in a Bayesian manner over the course of pursuit. They made use of a novel experimental paradigm, with 1D and 2D motion signals signifying different stages of the timecourse of pursuit due to the known effects of the aperture problem phenomenon. However, they, like Orban de Xivry (2013), blanked the target at certain time intervals to change the uncertainty of the motion. While the current work also suggests a dynamic reweighting of prior and likelihood over the course of pursuit, it was able to show how the timecourse of this reweighting changed as a function of increased variability in both the prior and likelihood. Additionally, the prior in Bogadhi et al. (2013) was initially set to 0, due to the belief of a prior favoring slow and smooth motion. The current study assumes the prior was learned experimentally over the course of many trials.

More recently, the model of Darlington, Tokiyama, & Lisberger (2017) looked at the effect of speed and direction context on smooth pursuit. They were able to show a strong bias in pursuit speed or direction due to the context of the properties of target motion on either the immediately preceding trial or the statistical properties of the block of trials. The observed bias due to context depended on the contrast of the target, with the lower-contrast targets resulting in a greater influence of the context on pursuit. However, they only looked at one specific time interval of pursuit (50-100 ms after the onset of pursuit) rather than the entire timecourse. Additionally, the decrease of contrast, while associated with a reduction of the firing rate of populations of neural responses in MT (Yang et al., 2012; Krekelberg et al., 2006) may not necessarily be the best measure of uncertainty in a moving target. This is especially true for analyses of pursuit direction, in which there is little documented effect of contrast. In contrast, the current study uses directional variability as a measure of uncertainty in the visual stimulus and analyzes pursuit across the entire timecourse of the trial.

Another recent study that approached smooth pursuit as a process related to Bayesian cue combination was by Deravet et al. (2018). The moving stimulus was either a disc or a 2D Gaussian blob. They defined two types of trials, training and test. Training trials consisted of a sequence of 1-5 trials with same stimulus velocity. Test trials had stimulus velocities which were higher or lower than those in the training trials. They found that increasing the number of repetitions of a given stimulus velocity in the training trials lead to a greater bias in eye velocity on test trials toward the velocity of the training trials. The effect of the training trials was greater with the Gaussian blobs than with the disk.

The present study differs from the previous work described above in that the statistical properties of prior and likelihood were varied systematically using Gaussian distributions with a given mean and standard deviation, and in addition, the present study focused on pursuit direction. Directional properties of pursuit are not often studied (De'Sperati & Viviani, 1997) and the effects of directional noise on pursuit has been studied very little (Watamaniuk & Heinen, 1999; Mukherjee et al., 2017).

4.4. From Bayesian cue combination to a model of smooth pursuit

The current study included a test of a model for smooth pursuit reflecting the basic principles of Bayesian cue combination which, at least qualitatively, may have accounted for the tradeoff between anticipatory and sensory-driven aspects of the direction of smooth pursuit. However, the current work and model raise many more questions about the nature of the computational and neural integration of prior and likelihood signals. These issues would need to be addressed in future work before the current model can be evolved into a complete model of pursuit.

First: the model does not account for the directional variability of pursuit. For example, if the output of the model is interpreted to represent the direction of pursuit at a given time interval, then we would expect that the standard deviation of the posterior resulting from the weighted combination of prior and likelihood would be related to the directional variability of pursuit direction. However, based on the estimates of the standard deviation of pursuit direction predicted by the posterior (based on the variance of the prior and the estimated variance of the likelihood, σ_s: $\sigma_{post}^2 = \frac{\sigma_P^2 \sigma_s^2}{\sigma_P^2 + \sigma_s^2}$) would predict a greater difference between the directional variability of pursuit for each value of

σ_L. For instance, when σ_s was estimated to be 0 for subject JG in Experiment 2 (Fig. 2.7), the calculation of the standard deviation of the posterior would predict directional variability of 0° in pursuit, which is physically impossible. There would realistically have to be some noise, whether it is in perception, the eye, or measurement, that is contributing to variability in pursuit. Thus, the current model cannot be accurately incorporating sources of variability in σ_s. Future models could adopt the approach of Yin et al. (2019) and include a parameter representing the baseline noise in the system. A strong test of the model of Bayesian cue combination would involve (as in Yin et al., 2019) an independent estimate of the noise parameter that would be able to accurately predict the standard deviation of the posterior.

Second: how would the dynamics of pursuit fit into the current model? The current model computes an estimate of pursuit direction at each time interval independently given a few parameters related to the nominal properties of the prior and stimulus. In reality, once the target begins to move, the pursuit response is likely to be affected by processes at different neural levels (including low levels) that affect the kinematic properties of the response to the immediate retinal error. Thus, as with both classical (Robinson, 1984; Krauzlis & Lisberger, 1994) and recent (Orban de Xivry et al., 2013) attempts, a full model of pursuit would need to incorporate the dynamics and kinematics inherent in smooth pursuit. These attempts also should include the dynamics of changes in direction (desperate & Viviani, 1997). Future models could frame the output of Bayesian cue combination to be some belief about the direction of the target rather than eye velocity, with this belief being the input to some function which includes the dynamics and kinematics of smooth pursuit. This function would then output the

direction of pursuit. (For example: $\theta_e = f(\theta_b)$, where e = eye, and b = belief). Such models would also require a term for the representation of the target and eye velocity at each timestep to compute the retinal slip (the difference between the eye and target velocities). Therefore, a full model of pursuit would require that each time interval not be treated separately.

To develop a more realistic approach to pursuit over time, a model that incorporated the low-level factors along with Bayesian updating, where the prior of the current timestep would be based on the posterior from the previous timestep (e.g., Montagnini et al. 2007) would be a promising framework. Eq. 9 below presents a possible restructuring of the Bayesian cue combination model adapted from Kording & Wolpert (2004). The model only explicitly includes the prior on the first timestep and integrates the likelihood with the posterior from the last timestep on each subsequent timestep.

$$\text{Time} = 0 \text{ ms: } \theta_{e,0} = \frac{\sigma_{s,0}^2}{\sigma_P^2 + \sigma_{s,0}^2}\mu_P + \frac{\sigma_P^2}{\sigma_P^2 + \sigma_{s,0}^2}\mu_s$$

$$\text{Time} > 0 \text{ ms (t): } \theta_{e,t} = \frac{\sigma_{s,t}^2}{\sigma_{e,t-1}^2 + \sigma_{s,t}^2}\theta_{e,t-1} + \frac{\sigma_{e,t-1}^2}{\sigma_{e,t-1}^2 + \sigma_{s,t}^2}\mu_s$$

$$\text{For any t: } \sigma_{e,t-1}^2 = \frac{\sigma_{s,t-1}^2\sigma_{e,t-2}^2}{\sigma_{s,t-1}^2 + \sigma_{e,t-2}^2}$$

Equation 9

Here, $\theta_{e,t}$ represents the direction of pursuit at time t, and $\sigma_{e,t-1}^2$ is the variance of the estimate of the direction of pursuit from the previous timestep. All other parameters are the same as in Eq. 8.

Another important issue raised by the present results is where the "extraretinal" cues (priors) are represented in the brain. There are plenty of neural candidates. Area MT is home to the representation of image motion, making it an obvious place for information related to the sensory likelihood (motion of the target) to originate, with the population of neurons in MT corresponding to certain speeds (or possibly directions) responding with higher firing rates when the motion stimulus is more reliable (Krekelberg et al., 2006). The location of the representation of the prior is a bit more ambiguous. "Extraretinal" signals have long been a component of models of predictive pursuit (Barnes & Collins, 2008; Bogadhi et al., 2013; Orban de Xivry et al., 2013), but the term has generally been used as a catch-all for inputs to pursuit that are not reliant on incoming sensory information rather than any specific neural signal. Possible origins of this extraretinal include prefrontal cortex (which sends signals to MT), FEF (specifically, the frontal pursuit area), or SEF (Lisberger, 2010; Kowler et al., 2019; Heinen & Liu, 1997; de Hemptinne et al., 2008). As mentioned before, pursuit is also suspected of being influenced by a corollary discharge signal representing the motor command executed in a previous timestep that is used as in input to pursuit. In the present experiment this motor command, to some extent, may be seen as embodying the influence of the prior and thus a separate "memory" for the prior might not be needed.

Where (and how) might the integration of the prior and likelihood cues actually take place? The integration may occur at the sensory or motor level, effecting in addition to pursuit the perception of the direction of motion due to activity in MT or MST, or affecting the later stages of pursuit further downstream (perhaps the frontal pursuit area). On the other hand, the perceptual results of Experiment 6 in the current study show an

effect of the directional noise of the RDK on the weights of the prior and likelihood with similar trends to the pursuit results (Experiments 1-4 and 5), suggesting that the combination process may be occurring at the perceptual and not exclusively the oculomotor level. Once combined, the relative strength of each cue may be determined by the difference in firing rates, with the likelihood taking some time to fully overtake the prior. Alternatively, the graded transition from prior to likelihood could be related to the rotation of population vectors in MT, with it taking some time for the perception of motion or pursuit to change direction. In the case of the wide prior ($\sigma_P = 45°$), the larger directional error earlier in pursuit may lead to a corrective pursuit response that starts earlier.

In addition to the above issues, future models should also consider the independence of the prior and likelihood. Since the mean of the likelihood on each trial is drawn from the prior, the likelihood is dependent on the mean of the prior. Traditionally, models of Bayesian cue combination have an underlying assumption that the two cues are independent. Since this does not hold in the current experimental paradigm, the model will likely need to be modified to account for the dependence of likelihood on the prior. Adding a discounting term for the correlation between the two cues may be sufficient for computing a combination of correlated cues (Oruc, Maloney, & Landy, 2003). Another source of non-independence is learning. In the case of pursuit with the narrow prior, the pursuit of similar directions of motions in the same block of trials could lead to improved tuning of responses at the sensory or motor levels. An experiment that used a perceptual cue on each trial to signal the likely direction of

upcoming motion (similar in some ways to Santos & Kowler, 2017) could preserve the benefits of the prior while reducing the role of repetition and learning.

Finally, future models should be tested on different priors, including a bimodal prior to test the role of the overt ASEM found at the onset of target motion. A bimodal prior is likely to suppress the ASEM. At the same time, previous work in motor control has shown that participants are able to learn more complex priors, including bimodal priors, and still combine the prior with the likelihood in a Bayesian way (Kording & Wolpert, 2004). A bimodal prior with each mode 180° apart would still provide higher-level information about the possible directions of the sensory likelihood without the overt effects of ASEM at the onset of target motion.

4.5. Clinical implications

Aside from the enhancing our understanding of the neural and computational properties of predictive smooth pursuit, the current work also has some potential clinical applications. Predictive and anticipatory smooth pursuit has been found to be impaired in individuals with Parkinson's disease (Fukushima et al., 2017; Helmchen, 2012). Additionally, difficulties in anticipatory pursuit has been suggested to be a marker for schizophrenia (Avila et al., 2006) and the psychotic components of some affective disorders such as bipolar disorder (Brakemeier et al., 2019). While not specifically aimed at clinical populations, the current experimental paradigm could help develop in developing a computational framework to quantify the deficits in prediction during pursuit that may be present in these disorders.

Recent work in computational psychiatry proposes the framing psychiatric disorders as failures in one or more aspects of a Bayesian theoretic objective function used to make decisions (Huys, et al., 2015). For instance, when making a decision, the terms of the observer's objective function, mechanisms carrying out the function, or other inputs to the function may be at fault. Framing the integration of prior and likelihood in pursuit described by this study as the objective function controlling the pursuit process could allow for a similar analysis in the current experimental setup. Specifically, isolating properties of the prior and likelihood related to the impairment of pursuit within the current study's experimental paradigm and future iterations of the Bayesian model may be useful in quantifying aspects of the disorders (Parkinson's or schizophrenia for example) that result in impaired pursuit.

4.6. Final conclusions and implications

For over 50 years, smooth pursuit eye movements have been known to use non-sensory information predict future target motion. However, up until recently, the effects of higher-level extraretinal signals on pursuit over the timecourse of pursuit was rarely quantified statistically. Recent work has made strides in modeling anticipatory smooth pursuit and has suggested that predictive pursuit may operates by means of optimal Bayesian combination of prior (extraretinal) and likelihood (sensory) cues, as has similarly been demonstrated for other perceptual and motor processes. The current study opens doors for further experimentation and modeling by showing that the direction of pursuit may be determined by an optimal combination of sensory and extraretinal influences across the timecourse of pursuit, rather than at one specific, early stage of

pursuit. This influence of prior and likelihood was shown to be modulated by changes in the directional variability of each. There was also a dependence of the variability of pursuit direction on the directional variability of prior and likelihood. As the more reliable prior and likelihood resulted in lower directional pursuit variability, a possible role of prediction in reducing the effects of stimulus noise on the variability of pursuit was proposed. Future work will be needed to develop the proposed Bayesian cue combination model and hone in on the neural areas involved.

5. References

Heinen, S. J., & Liu, M. (1997). Single-neuron activity in the dorsomedial frontal cortex during smooth-pursuit eye movements to predictable target motion. Visual Neuroscience, 14(5), 853–865. https://doi.org/10.1017/S0952523800011597

Berens, P. (2009). CircStat: A MATLAB Toolbox for Circular Statistics. Wiley Interdisciplinary Reviews: Computational Statistics, 1(1), 128–129. https://doi.org/10.1002/wics.10

Kowler, E., & Steinman, R. M. (1979). The effect of expectations on slow oculomotor control-I. Periodic target steps. Vision Research, 19(6), 619–632. https://doi.org/10.1016/0042-6989(79)90238-4

Bogadhi, A. R., Montagnini, A., Mamassian, P., Perrinet, L. U., & Masson, G. S. (2011). Pursuing motion illusions: A realistic oculomotor framework for Bayesian inference. Vision Research, 51(8), 867–880. https://doi.org/10.1016/j.visres.2010.10.021

Dakin, S. C., Mareschal, I., & Bex, P. J. (2005). Local and global limitations on direction integration assessed using equivalent noise analysis. Vision Research, 45(24), 3027–3049. https://doi.org/10.1016/j.visres.2005.07.037

Barnes, G. R., & Collins, C. J. S. (2008). Evidence for a Link Between the Extra-Retinal Component of Random-Onset Pursuit and the Anticipatory Pursuit of Predictable Object Motion. Journal of Neurophysiology, 100(2), 1135–1146. https://doi.org/10.1152/jn.00060.2008

Weiss, Y., Simoncelli, E. P., & Adelson, E. H. (2002). Motion illusions as optimal percepts. Nature Neuroscience, 5(6), 598–604. https://doi.org/10.1038/nn858

Krauzlis, R. J., & Lisberger, S. G. (1994). A model of visually-guided smooth pursuit eye movements based on behavioral observations. Journal of Computational Neuroscience, 1(4), 265–283. https://doi.org/10.1007/BF00961876

Fukushima, K., Fukushima, J., & Barnes, G. R. (2017, May 3). Clinical application of eye movement tasks as an aid to understanding Parkinson's disease pathophysiology. Experimental Brain Research. Springer Berlin Heidelberg. https://doi.org/10.1007/s00221-017-4916-5

Orban de Xivry, J.-J., Coppe, S., Blohm, G., & Lefevre, P. (2013). Kalman Filtering Naturally Accounts for Visually Guided and Predictive Smooth Pursuit Dynamics. Journal of Neuroscience, 33(44), 17301–17313. https://doi.org/10.1523/JNEUROSCI.2321-13.2013

Kowler, E., & Steinman, R. M. (1979). The effect of expectations on slow oculomotor control-II. Single target displacements. Vision Research, 19(6), 633–646. https://doi.org/10.1016/0042-6989(79)90239-6

Helmchen, C., Pohlmann, J., Trillenberg, P., Lencer, R., Graf, J., & Sprenger, A. (2012). Role of anticipation and prediction in smooth pursuit eye movement control in Parkinson's disease. Movement Disorders, 27(8), 1012–1018. https://doi.org/10.1002/mds.25042

Groh, J. M., Born, R. T., & Newsome, W. T. (1997). How is a sensory map read Out? Effects of microstimulation in visual area MT on saccades and smooth pursuit eye movements. The Journal of Neuroscience, 17(11), 4312–4330.

Oruç, I., Maloney, L. T., & Landy, M. S. (2003). Weighted linear cue combination with possibly correlated error. Vision Research, 43(23), 2451–2468. https://doi.org/10.1016/S0042-6989(03)00435-8

Bogadhi, A. R., Montagnini, A., & Masson, G. S. (2013). Dynamic Interaction between retinal and extra-retinal signals in motion integration for smooth pursuit. Submitted, 13(13), 5. https://doi.org/10.1167/13.13.5

Kowler, E., & McKee, S. P. (1987). Sensitivity of smooth eye movement to small differences in target velocity. Vision Research. https://doi.org/10.1016/0042-6989(87)90014-9

Ma, W. J. (2012, October 1). Organizing probabilistic models of perception. Trends in Cognitive Sciences. Elsevier Current Trends. https://doi.org/10.1016/j.tics.2012.08.010

Kowler, E., Rubinstein, J. F., Santos, E. M., & Wang, J. (2019). Predictive Smooth Pursuit Eye Movements. Annual Review of Vision Science, 5(1), 223–246. https://doi.org/10.1146/annurev-vision-091718-014901

Yin, C., Wang, H., Wei, K., & Körding, K. P. (2019). Sensorimotor priors are effector dependent. Journal of Neurophysiology, 122(1), 389–397. https://doi.org/10.1152/jn.00228.2018

De'Sperati, C., & Viviani, P. (1997). The relationship between curvature and velocity in two-dimensional smooth pursuit eye movements. Journal of Neuroscience, 17(10), 3932–3945. https://doi.org/10.1523/JNEUROSCI.17-10-03932.1997

Körding, K. P., & Wolpert, D. M. (2004). Bayesian integration in sensorimotor learning. Nature, 427(6971), 244–247. https://doi.org/10.1038/nature02169

Mukherjee, T., Liu, B., Simoncini, C., & Osborne, L. C. (2017). Spatiotemporal Filter for Visual Motion Integration from Pursuit Eye Movements in Humans and Monkeys. The Journal of Neuroscience, 37(6), 1394–1412. https://doi.org/10.1523/JNEUROSCI.2682-16.2016

Borghuis, B. G., & Leonardo, A. (2015). The Role of Motion Extrapolation in Amphibian Prey Capture. Journal of Neuroscience, 35(46), 15430–15441. https://doi.org/10.1523/JNEUROSCI.3189-15.2015

Avila, M. T., Hong, L. E., Moates, A., Turano, K. A., & Thaker, G. K. (2006). Role of anticipation in schizophrenia-related pursuit initiation deficits. Journal of Neurophysiology, 95(2), 593–601. https://doi.org/10.1152/jn.00369.2005

Kowler, E. (1989). Cognitive expectations, not habits, control anticipatory smooth oculomotor pursuit. Vision Research, 29(9), 1049–1057. https://doi.org/10.1016/0042-6989(89)90052-7

Robinson, D. A., Gordon, J. L., & Gordon, S. E. (1986). A Model of the Smooth Pursuit Eye Movement System. Biol. Cybern, 55, 43–57. https://doi.org/10.1007/BF00363977

Kowler, E., Martings, A. J., & Pavel, M. (1984). Anticipatory Smooth Eye Movements Depend on Prior Target Motions. Vision Research, 24(3), 197–210.

Darlington, T. R., Beck, J. M., & Lisberger, S. G. (2018). Neural implementation of Bayesian inference in a sensorimotor behavior. Nature Neuroscience, 21(10), 1442–1451. https://doi.org/10.1038/s41593-018-0233-y

Deravet, N., Blohm, G., de Xivry, J.-J. O., & Lefèvre, P. (2018). Weighted integration of short-term memory and sensory signals in the oculomotor system. Journal of Vision, 18(5), 16. https://doi.org/10.1167/18.5.16

Brakemeier, S., Sprenger, A., Meyhöfer, I., McDowell, J. E., Rubin, L. H., Hill, S. K., … Lencer, R. (2019). Smooth pursuit eye movement deficits as a biomarker for psychotic features in bipolar disorder - Findings from the PARDIP study. Bipolar Disorders, bdi.12865. https://doi.org/10.1111/bdi.12865

Dallos, P. J., & Jones, R. W. (1963). Learning Behavior of the Eye Fixation Control System. IEEE Transactions on Automatic Control, 8(3), 218–227. https://doi.org/10.1109/TAC.1963.1105574

De Hemptinne, C., Lefèvre, P., & Missal, M. (2006). Influence of cognitive expectation on the initiation of anticipatory and visual pursuit eye movements in the rhesus monkey. Journal of Neurophysiology, 95(6), 3770–3782. https://doi.org/10.1152/jn.00007.2006

Rucci, M., & Victor, J. D. (2015). The unsteady eye: an information-processing stage, not a bug. Trends in Neurosciences, 38(4), 195–206. https://doi.org/10.1016/j.tins.2015.01.005

Watamaniuk, S. N. J., & Heinen, S. J. (1999). Human smooth pursuit direction discrimination. Vision Research, 39(1), 59–70. https://doi.org/10.1016/S0042-6989(98)00128-X

Santos, E. M., & Kowler, E. (2017). Anticipatory smooth pursuit eye movements evoked by probabilistic cues. Journal of Vision, 17, 1–16. https://doi.org/10.1167/17.13.13.doi

Darlington, T. R., Tokiyama, S., & Lisberger, S. G. (2017). Control of the strength of visual-motor transmission as the mechanism of rapid adaptation of priors for Bayesian inference in smooth pursuit eye movements. Journal of Neurophysiology, 118(2), 1173–1189. https://doi.org/10.1152/jn.00282.2017

Mukherjee, T., Battifarano, M., Simoncini, C., & Osborne, L. C. (2015). Shared Sensory Estimates for Human Motion Perception and Pursuit Eye Movements. Journal of Neuroscience, 35(22), 8515–8530. https://doi.org/10.1523/JNEUROSCI.4320-14.2015

Ernst, M. O., & Banks, M. S. (2002). Humans integrate visual and haptic information in a statistically optimal fashion. Nature, 415(6870), 429–433. https://doi.org/10.1038/415429a

Ladda, J., Eggert, T., Glasauer, S., & Straube, A. (2007). Velocity scaling of cue-induced smooth pursuit acceleration obeys constraints of natural motion. Experimental Brain Research, 182(3), 343–356. https://doi.org/10.1007/s00221-007-0988-y

Montagnini, A., Mamassian, P., Perrinet, L., Castet, E., & Masson, G. S. (2007). Bayesian modeling of dynamic motion integration. Journal of Physiology Paris, 101(1–3), 64–77. https://doi.org/10.1016/j.jphysparis.2007.10.013

Lisberger, S. G. (2010, May 27). Visual guidance of smooth-pursuit eye movements: Sensation, action, and what happens in between. Neuron. Elsevier. https://doi.org/10.1016/j.neuron.2010.03.027

Westheimer, G. (1954). Eye movement responses to a horizontally moving visual stimulus. A.M.A. Archives of Ophthalmology, 52(6), 932–941. https://doi.org/10.1001/archopht.1954.00920050938013

Becker, W., & Fuchs, A. F. (1985). Prediction in the oculomotor system: smooth pursuit during transient disappearance of a visual target. Experimental Brain Research, 57(3), 562–575. https://doi.org/10.1007/BF00237843

Trommershauser, J., Maloney, L. T., & Landy, M. S. (2003). Statistical decision theory and trade-offs in the control of motor response. Spat.Vis., 16(3–4), 255–275. https://doi.org/10.1163/156856803322467527

Watamaniuk, S. N. J., Sekuler, R., & Williams, D. W. (1989). Direction perception in complex dynamic displays: The integration of direction information. Vision Research, 29(1), 47–59. https://doi.org/10.1016/0042-6989(89)90173-9

Yang, J., Lee, J., & Lisberger, S. G. (2012). The Interaction of Bayesian Priors and Sensory Data and Its Neural Circuit Implementation in Visually Guided Movement. Journal of Neuroscience, 32(49), 17632–17645. https://doi.org/10.1523/JNEUROSCI.1163-12.2012

Tassinari, H., Hudson, T. E., & Landy, M. S. (2006). Combining Priors and Noisy Visual Cues in a Rapid Pointing Task. Journal of Neuroscience, 26(40), 10154–10163. https://doi.org/10.1523/JNEUROSCI.2779-06.2006

Huys, Q. J. M., Guitart-Masip, M., Dolan, R. J., & Dayan, P. (2015). Decision-Theoretic Psychiatry. Clinical Psychological Science, 3(3), 400–421. https://doi.org/10.1177/2167702614562040

Krekelberg, B. (2006). Interactions between Speed and Contrast Tuning in the Middle Temporal Area: Implications for the Neural Code for Speed. Journal of Neuroscience, 26(35), 8988–8998. https://doi.org/10.1523/JNEUROSCI.1983-06.2006

Sato, Y., & Kording, K. P. (2014). How much to trust the senses: Likelihood learning. Journal of Vision, 14(13), 13–13. https://doi.org/10.1167/14.13.13

Orban de Xivry, J. J., Missal, M., & Lefevre, P. (2008). A dynamic representation of target motion drives predictive smooth pursuit during target blanking. Journal of Vision, 8(15), 6–6. https://doi.org/10.1167/8.15.6